

Temperature calculations in fire exposed structures with the use of adiabatic surface temperatures

Joakim Sandström

Luleå tekniska universitet
Civilingenjörsprogrammet
Brandteknik
Institutionen för Samhällsbyggnad
Avdelningen för Byggnadsmekanik

Preface

CFD simulations take time. That's why this work is made, to save time. But it takes time to save time and that is something I have learned.

This work has been carried out at SP - Swedish National Testing and Research Institute in Borås and at the division of Structural Engineering at LTU, Luleå University of Technology.

Many persons have helped me in finishing this work and I cannot thank all of them enough. Among the persons to thank are my supervisor professor Ulf Wickström for allowing me to do this work at SP and Lars Bernspång who has been supporting all the way. I had a great week at SP in Borås and want to thank Maria and Heimo for helping me with the softwares, Robert for questioning everything and Bijan for helping me with computer resources. I also want to thank Henrik at LTU for sharing computer resources and Ibrahim and Allan for helpful comments.

Finally I want to thank Erika for all the support and the rest my family to whom I owe it all.

Karlstad, February 2008

A handwritten signature in black ink, appearing to read 'Joakim', written in a cursive style.

Joakim

Abstract

Fire safety engineering is offering more and more advanced methods including software for fire dynamic calculations. This thesis presents a method for using the results obtained by fire modelling using the code FDS (Fire Dynamic Simulator) as input to FEM calculations for predicting temperature in fire exposed structures.

Prof. Wickström of SP Sweden has introduced the concept of adiabatic surface temperature (AST) for calculating heat transfer to fire exposed structures. The AST is defined as the temperature of a surface which cannot absorb any energy.

It may be calculated at any surface in the fire simulation software used in this thesis. The aim in this work is to see if the AST at the surface of a beam in one simulation gives satisfactory temperature result when used in a temperature calculation of beams with different dimensions.

The work is divided into four parts. The first part is to validate the AST as a means for calculations of temperature in fire exposed structures. Using the AST in the calculations presented an almost perfect agreement with the temperature obtained directly from the CFD code.

The second part is a comparison made to investigate whether AST calculated by FDS could be used in a FEM simulation to predict heat transfer to a fire exposed structure.

As the third part some different simulations are run to compare the FEM temperature calculations of beams with AST from different simulations.

The result showed that AST obtained in one fire scenario can be used for different beam sections. It is advised to use the technique with care since certain circumstances such as choice of convection coefficients and flame height can influence the results.

The final part is to make an experimentally verifiable set up. This is made to be able to compare simulated results with tests to be made at SP and at ULC in Canada. The result of that is presented as an input file to FDS in the appendix.

Sammanfattning

Till hjälp för dagens brandingenjörer kommer mer och mer avancerade hjälpmedel. Ett av dessa hjälpmedel är bland annat mjukvara för brandsimuleringar. I det här arbetet presenteras en metod för användandet av utdata från brandsimuleringar i FDS (Fire Dynamic Simulator) som indata i FEM-baserade temperaturberäkningar i brandutsatta konstruktioner.

Prof. Wickström på SP i Borås har som hjälp inom temperaturberäkningar av brandutsatta konstruktioner introducerat adiabatiska yttemperaturer (AST). Den adiabatiska yttemperaturen är den temperatur på en yta då värmeflödet över ytan är noll.

FDS kan beräkna den adiabatiska yttemperaturen på alla ytor i en simulering och målet med det här examensarbetet är se om AST från en simulering kan användas i temperaturberäkningar på ett element med andra dimensioner än de som använts i simuleringen.

Rapporten är delad i fyra delar där den första delen kontrollerar användandet av AST genom att göra en temperaturberäkning i en stålplatta. T_{AST} används i en handberäkningsmodell som ersättning för T_f och temperaturberäkningarna visade det en nästan perfekt överensstämmelse med temperaturen beräknad direkt i FDS.

I den andra delen testas det tvådimensionella fallet genom att AST från FDS används i en FEM-beräkning för att beräkna värmeflödet till ett brandutsatt element.

Som tredje del jämförs temperaturberäkningar i FEM med AST från olika simuleringar.

Resultaten visar att AST från en brandsimulering kan användas i temperaturberäkningar på balkar med olika dimensioner. Metoden bör dock användas med försiktighet då omständigheter så som flamhöjd och val av konvektionskoefficient påverkar resultaten.

Den fjärde och sista delen handlar om att skapa en FDS-modell vars beräkningar kommer att jämföras med fullskaliga experiment gjorda på SP i Borås och ULC i Kanada. Resultatet därifrån presenteras som en FDS-fil i bilaga B.

TABLE OF CONTENT

PREFACE	I
ABSTRACT	II
SAMMANFATTNING	IV
SYMBOLS	1
1 INTRODUCTION	3
1.1 BACKGROUND AND IDENTIFICATION OF THE PROBLEM	3
1.2 AIM.....	4
1.3 LIMITATIONS	4
1.4 METHOD	4
2 FIRE CALCULATIONS	6
2.1 HEAT TRANSFER	6
2.2 DESIGN FIRE TEMPERATURE.....	10
2.3 PLATE THERMOMETER	12
2.4 ADIABATIC SURFACE TEMPERATURE	13
2.5 SPREAD SHEET CALCULATIONS OF STEEL TEMPERATURE.....	14
3 SOFTWARE	16
3.1 INTRODUCTION TO CFD AND FDS.....	16
3.2 INTRODUCTION TO FEM AND TASEF.....	18
4 RESULTS	21
4.1 VERIFICATION OF AST WITH SPREAD SHEET CALCULATIONS VIA THE VERIFICATION OF STEEL TEMPERATURE CALCULATED IN FDS	21
4.2 CALCULATION OF BEAM TEMPERATURE WITH TASEF.....	26
4.3 VERIFICATION OF THE USE OF AST IN HEAT TRANSFER CALCULATIONS	30
4.4 SETUP OF A FIRE SCENARIO THAT CAN BE EXPERIMENTALLY VERIFIED.....	39
5 CONCLUSIONS AND FURTHER RESEARCH	54
APPENDIX A	A
APPENIX B	C

Symbols

Latin upper case letters

A_s	Area of perimeter per unit length of steel beam [m^2]
$\bar{\mathbf{K}}$	Thermal conductivity matrix [W/K]
L	Length of surface exposed to convection [m]
$\bar{\mathbf{Q}}$	Heat flux vector [W]
Q_i	Nodal heat flux [W]
Q	Internally generated heat [W/m^3]
$\bar{\mathbf{T}}$	Node temperature vector [K]
T_g	Convective or gas temperature [K]
T_r	Radiative temperature [K]
T_f	Fire temperature [K]
T_{AST}	Adiabatic surface temperature [K]
V_s	Volume of steel beam per unit length [m^3]

Latin lower case letters

c_p	Specific heat capacity [J/kgK]
e	Specific volumetric enthalpy [J/m^3]
h	Convective heat transfer coefficient [$\text{W/m}^2\text{K}$]
k	Thermal conductivity [W/mK]
l	Length of element [m]
\dot{q}''_{con}	Heat flux from convection [W/m^2]
$\dot{q}''_{conductive}$	Heat flux from conduction [W/m^2]
\dot{q}''_{emi}	Heat flux emitted from surface [W/m^2]
\dot{q}''_{inc}	Incoming heat flux to a surface [W/m^2]
\dot{q}''_{rad}	Radiative heat flux [W/m^2]
\dot{q}''_{tot}	Total heat flux [W/m^2]

t	Time [s]
x, y	Coordinates [m]

Greek lower case letters

α_s	Radiation absorptivity [-]
ε	Emissivity [-]
ϕ	View factor [-]
μ	Viscosity [Pa s]
ρ	Density [kg/m ³]
σ	Stefan Boltzmann's constant [W/m ² K ⁴]
τ	Variable used in beam temperature calculations [s]
ν_s	Mean fluid velocity [m/s]
ν	Kinematic viscosity [m ² /s]

1 Introduction

1.1 Background and identification of the problem

Fire engineering is offering more and more advanced methods. In construction, software makes it easy to calculate the progress of an assumed fire and temperature effect on construction elements such as beams. A general problem is the unbalance in computational time between fire simulations and FEM calculations. To get the boundary conditions for a rather simple FEM-calculation it could be necessary to run a fire simulation for weeks. If the construction element is changed, a new fire simulation is needed. This problem could be solved with the possibility to simulate a general scenario for the situation surrounding a construction element rather than the exact conditions for each different construction element.

NIST [1] has developed a CFD-code (Computational Fluid Dynamic) called FDS (Fire Dynamic Simulator) [2]. This software is made for calculating fire development in different scenarios. In a given scenario FDS can calculate the heat transfer and temperature of construction elements in one dimension. This temperature can be used in FEM-calculations but is limited to the construction element used in that particular fire simulation thus not solving the problem of usability in different FEM calculations in one, two or three dimensions.

When working with temperature calculations in fire exposed structures Professor Ulf Wickström [3] of SP - Technical Research Institute of Sweden introduced the concept of adiabatic surface temperatures, T_{AST} or AST [4]. This temperature can be measured with a very thin steel plate with insulation as backing considering both the radiation and convection. This is necessary to calculate temperature of elements exposed to fire. The concept of AST is possible to use in almost any scenario or experimental set up of fire exposed

structures but is it possible to use in a simulated environment. What are the difficulties?

Is the concept of AST a method for defining fire environments which can facilitate FEM temperature calculations and save much computational efforts? This thesis is an attempt to answer that question.

1.2 Aim

The aim of this thesis is to test AST as a possible input in temperature calculations of beams. Also to test the ability to use AST calculated in CFD - simulations as a fire environment that can be used in FEM calculations on different construction set ups. Finally create a model that can be verified with an experiment at SP – Research Institute of Sweden.

1.3 Limitations

This thesis is purely theoretical and is based on computer simulations. No experiments are made although a model is developed that can be verified experimentally.

1.4 Method

This work can be divided into four major parts. The first part presented in chapter 2 and 3 is a theoretical overview of the areas covered in this thesis. These chapters deals with heat transfer, traditional post flashover temperature calculations and finally gives a brief introduction to the FDS and TASEF codes.

The second part in chapter 4.1 is dealing with the verification of AST as an input method for temperature calculation in FEM software. The first step to verify AST is to compare a relatively simple spread calculation method using AST as input with the steel temperature calculated directly in the fire simulation software FDS.

After that a test is made in chapter 4.2 to see if it is possible to use AST as an boundary input in the two - dimensional temperature FEM software code TASEF. This is done since AST depends on surface orientation and needs to be prescribed with different values to different boundaries.

The third part presented in chapter 4.3 is the set up of scenarios designed to compare results of temperature calculations in TASEF with AST calculated in FDS as input. The different simulations are made to four different cases where AST could be used. The first case generates AST from a fire simulation with one beam. The values of AST are then used to calculate the temperature on a second beam with assumed same fire conditions. This is made to see if AST from one simulation is useable in FEM calculations with different a construction element.

If the first case is designed to compare different beams with the same fire scenario the second case is where the beam is identical but the fire scenario is different. The third case is made to see if it is possible to measure AST in a simulation without beam and compare the calculated temperature values from the simulation without beam to the temperature values calculated from the simulation with a beam.

The fourth case is an extra verification of the first case with similar fire scenario but different beams. This time it is made with lower effect from the energy source.

The fourth major part in the thesis is to create an experimentally verifiable FDS model that can give result to compare with full scale experiment to be performed at SP and ULC in Canada later on.

2 Fire calculations

2.1 Heat transfer

There are three different types of heat transfer; convection, radiation and conduction and the heat transferred to a point on a surface or object is the sum of all three of them. [5]

$$\dot{q}''_{tot} = \dot{q}''_{rad} + \dot{q}''_{conv} + \dot{q}''_{cond} \quad \text{Eq. 1}$$

In fire engineering the main focus is on convection and radiation and it is possible to assume no contribution of heat transfer from conduction.

2.1.1 Radiation

Heat transferred by radiation to a surface from a fire is as shown in **Fel! Hittar inte referensskälla.** where \dot{q}''_{inc} is the incident radiative heat to the surface, \dot{q}''_{ref} the reflected radiation and \dot{q}''_{emi} the radiation emitted from the surface itself.

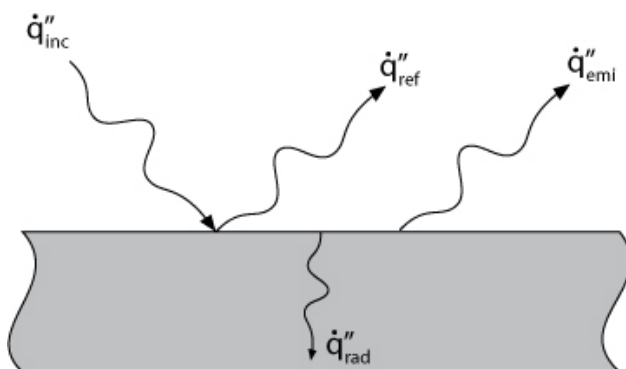


Figure 2-1 The heat transfer from radiation depends on \dot{q}''_{inc} , \dot{q}''_{ref} and \dot{q}''_{emi}

The net heat transfer to a surface is calculated as \dot{q}''_{rad} in Eq. 2.

$$\dot{q}''_{rad} = \alpha_s \dot{q}''_{inc} - \dot{q}''_{emi} \quad \text{Eq. 2}$$

Where α_s is the surface absorptivity and tells how much of \dot{q}_{inc}'' that actually contributes to \dot{q}_{rad}'' . \dot{q}_{emi}'' is depending on the surface emissivity, ε , and the surface temperature to the power of four as shown in Eq. 3.

$$\dot{q}_{emi}'' = \varepsilon \sigma T_s^4 \quad \text{Eq. 3}$$

The incoming radiation is based on the same equation but instead of sending radiation, the surface receives the radiation emitted from all the surrounding surfaces (see Eq. 4). In this case it is also important to consider the configuration [6] factors of all radiating surfaces in relation to the receiving surface.

$$\dot{q}_{inc}'' = \sum \varepsilon_i \phi_i \sigma T_i^4 \quad \text{Eq. 4}$$

This is difficult to calculate and it is more convenient to redefine Eq. 4 in some way. Stefan-Boltzmann's constant is taken out of the equation as it is the only value that is independent of the radiative surfaces. The sum of the radiative surfaces is then converted to one value, a theoretical temperature to the power of four that represents the temperature of a radiating black body with no configuration factor to consider. This temperature is defined as

$$T_r^4 = \sum \varepsilon_i \phi_i T_i^4 \quad \text{Eq. 5}$$

Combining Eq. 2, Eq. 3, Eq. 4, Eq. 5 and using Kirchhoff's identity saying $\varepsilon_s = \alpha_s$ gives us an easier way to present the net heat transfers from radiation where T_r and T_s represents the radiation temperature and structural element temperature respectively

$$\dot{q}_{rad}'' = \varepsilon_s \sigma (T_r^4 - T_s^4) \quad \text{Eq. 6}$$

2.1.2 Convection

Convection is the heat transfer from the media, in this case smoke or hot gas from the fire, in contact with the surface. The heat transfer is caused by the temperature difference between the temperature in the gas, T_g , and the structural temperature T_s . The difference is then multiplied with a convection coefficient, h , to obtain the heat flow from convection (see Eq. 7).

$$\dot{q}_{con}'' = h(T_g - T_s)^n \quad \text{Eq. 7}$$

The value n in Eq. 7 can vary but is usually simplified to 1 in fire calculations and is therefore omitted. There are different ways to calculate the convection coefficient and which method to use depends on if the type of flow is natural or forced and if the characteristic of the flow is laminar or turbulent.

2.1.2.1 Natural and Forced flow

There are two types of flow, natural and forced. The natural flow comes from flow created by temperature difference such as the buoyancy of air heated by a plate with no other interference. The flow is said to be forced if it's not temperature induced but rather forced by something else. Cold wind on a windy day is forced, hot air driven by a fire is also considered forced.

2.1.2.2 Laminar and turbulent flow

The other aspect of convection is the characteristics of the heat transporting media against the surface to which it transfers heat. A gentle and linear flow is considered laminar but if the flow on the other hand is chaotic it is said to be turbulent.

2.1.2.3 Convection in structural fire engineering

In fire dynamics the most common method for calculating convection is by assuming the flow to be forced and turbulent. The governing equation used to calculate the convection coefficient of a forced and turbulent flow analytically is Eq. 8.

$$h = \frac{k}{L} 0,037 \text{Re}^{\frac{4}{5}} \text{Pr}^{\frac{1}{3}} \quad \text{Eq. 8}$$

In addition to the thermal conductivity, k , and length, L , the variables used in Eq. 8 are the Reynolds and Prandtl numbers. Reynolds number (Eq. 9) depends on the mean velocity of the flowing media v_s , Length of the exposed surface L , and the kinematical viscosity of the flowing media ν .

$$\text{Re} = \frac{v_s L}{\nu} \quad \text{Eq. 9}$$

Prandtl's number is more concerned of the surface material and is derived from Eq. 10 where specific heat c_p and viscosity μ of the flowing media is divided by the thermal conductivity of the material.

$$\text{Pr} = \frac{c_p \mu}{k} \quad \text{Eq. 10}$$

The convective heat transfer coefficient, h , is then used as in Eq. 7 to calculate the amount of energy transferred from the fire to the construction element. In calculating convective heat transfer, \dot{q}_{con}'' , software such as FDS calculates h analytically using Eq. 8, Eq. 9 and Eq. 10 giving a h that vary over time depending on outcome of fire scenario. In regular fire temperature calculations

concerning steel the value is simplified to a constant assumed to be $h = 25$ W/m². [6]. This can lead to a problem when comparing results from fire simulations with temperature calculation methods since the analytical time varying h is not obtainable from fire simulations. This creates an uncertainty that can be seen further on in chapter 4.2.

This gives us a way to calculate the total heat flux in Eq. 1 as

$$\dot{q}_{tot}'' = \varepsilon_s \sigma (T_r^4 - T_s^4) + h(T_g - T_s) \quad \text{Eq. 11}$$

It is important to note that T_r and T_g are merely representations of the radiation and gas temperature at the surface of an object subjected to heat transfer from a fire scenario.

In most fire engineering cases T_r and T_g are assumed to be equal to one temperature that considers the heat transfer contribution from both radiation and convection. This temperature is referred to as the fire temperature or T_f and is an assumption made to simplify calculations and the value of T_f is always a value between the T_r and T_g .

$$\dot{q}_{tot}'' = \varepsilon_s \sigma (T_f^4 - T_s^4) + h(T_f - T_s) \quad \text{Eq. 12}$$

2.2 Design fire temperature

There are different ways of obtaining the post-flashover design fire temperature T_f . A common way is to represent T_f by different fire temperature curves. Four methods are briefly presented here.

- ISO 834 or EN 1363-1
- ASTM E-119
- The opening factor method
- Eurocode Parametric fires

ISO 834 (or EN 1363-1) and ASTM E-119 are the easiest ways to mimic the development of the fire temperature. ISO 834 is represented by an equation. ASTM E-119 is instead based on time temperature pairs with values similar to that of ISO 834. The ASTM E-119 and ISO 834 time – temperature relations are shown in Figure 2-2.

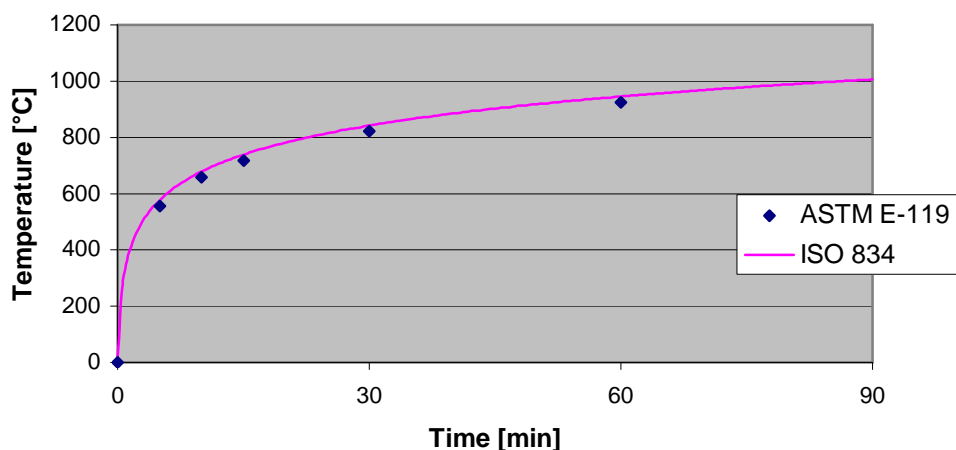


Figure 2-2 Time - temperature relations for structural fire safety engineering. Dark blue dots representing time temperature pairs as given in the American standard ASTM E-119. The purple line represents the international standard ISO 834 or the European EN 1363-1.

This way of describing a fire can be used when no other information is available. In an enclosure it is often possible to get more information concerning geometry and fire load. There are two variations of the ISO 834 fire curve depending on scenario. The hydro-carbon and external wall curves could be used where considered applicable.

The opening factor method uses information of fire load and the ventilation openings (see Figure 2-3).

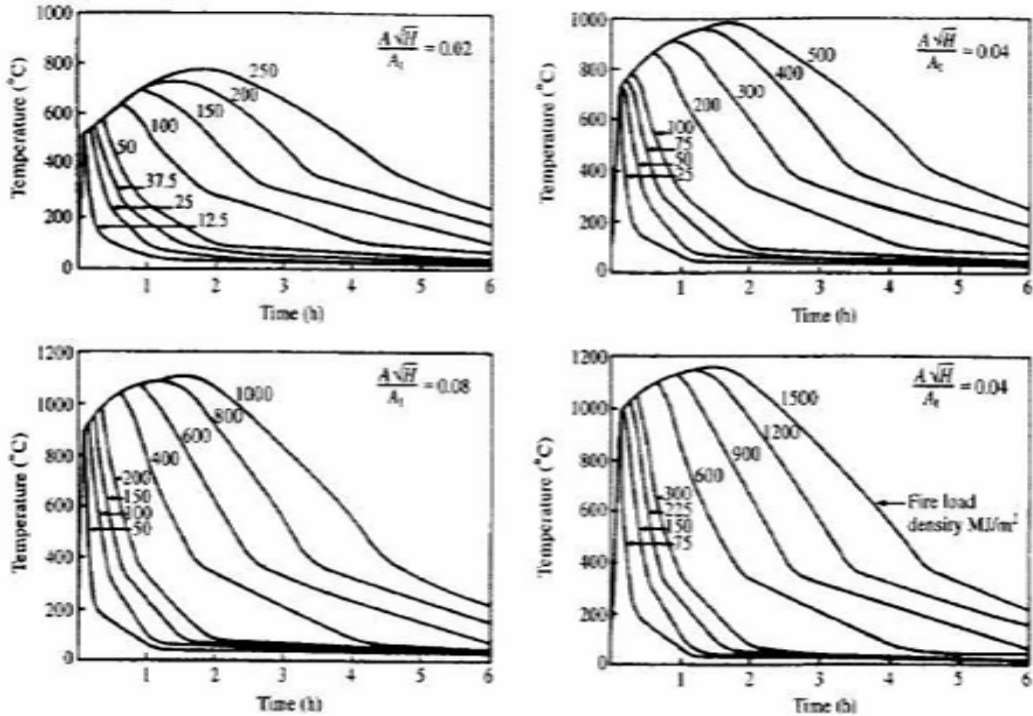


Figure 2-3 Time - temperature curves as described in the open factor method from [7].

The Eurocode parametric fire [8] gives an approximation of the opening factor method using an equation with parameters regarding geometry, fire load, ventilation and thermal properties of surrounding fire compartment surfaces.

2.3 Plate thermometer

When comparing temperature measurements from furnace fire resistance test all over Europe the conclusion that the normal way of measuring only with regard to gas temperature was insufficient. Large furnaces with a large mass of radiating, hot gas generated in general more onerous heating than small furnaces. To overcome this problem a device called the Plate Thermometer, PT, was developed by Ulf Wickström at SP. This device consists of a thin steel plate with a thermocouple and insulation on the back. This device is thin and reacts

fast on both radiation and convection assuming a temperature very close to that of an adiabatic surface.

2.4 Adiabatic Surface Temperature

An adiabatic surface temperature, T_{AST} is an ideal surface temperature where the transfer of heat into the surface equals the transfer out from the same. Thus T_{AST} is defined implicitly by Eq. 13 [4].

$$\varepsilon_s \sigma (T_r^4 - T_{AST}^4) + h(T_g - T_{AST}) = 0 \quad \text{Eq. 13}$$

Therefore T_{AST} must always lie between T_r and T_g letting the surface absorb energy from either radiation or convection and emit energy in the form of the other. At least one of the terms has to be negative to obtain zero heat flux as the sum of the parts. Both terms can also be zero given that $T_r = T_g$. In that case T_{AST} is equal to the temperature of T_r and T_g . T_{AST} will assume a value closer to the radiation temperature since the radiative heat transfer dominates at high temperatures occurring in fires.

An example can be made with temperatures $T_r = 800$ K and $T_g = 400$ K as input values in Eq. 13. Assuming the emissivity and convection coefficient to be $\varepsilon = 0.8$ and $h = 25$ W/m²K.

This gives an adiabatic surface temperature of $T_{AST} = 702.15$ K which is between T_r and T_g and closer to T_r . T_{AST} can be seen as a weighted average temperature regarding the radiation and convection temperature.

By combining equation Eq. 11 and Eq. 13, Eq. 14 can be derived. Thus T_r and T_g can be replaced by T_{AST} . T_{AST} can be obtained from both experiments (Plate Thermometer measurements) and computer simulations (CFD calculations).

$$\dot{q}_{tot}'' = \varepsilon_s \sigma (T_{AST}^4 - T_s^4) + h(T_{AST} - T_s) \quad \text{Eq. 14}$$

2.5 Spread sheet calculations of steel temperature

Spread sheet calculations of steel temperature using T_f can easily be adapted to the use of T_{AST} since they are exchangeable in calculations. The temperature change in steel is calculated and added to the last known temperature thus becoming the new known temperature for the next step in the calculation. This method is presented in Eq. 15 [9].

$$T_s^{i+1} = \frac{\Delta t}{\tau} T_{AST}^i + \left(1 - \frac{\Delta t}{\tau}\right) T_s^i \quad \text{Eq. 15}$$

The temperature calculations are based on some basic properties of the element subject to the calculation. Consideration is taken to the specific heat, c_s , density, ρ_s , slenderness in the form of the section factor and the heat transfer coefficient H . These properties are all represented in the variable τ explained in Eq. 16.

$$\tau = \frac{c_s \rho_s}{\left(\frac{A_s}{V_s}\right) H} \quad \text{Eq. 16}$$

The input of heat transferred from the fire is given in the variable H explained in Eq. 17. This is a rearrangement of Eq. 14 presented as an overall heat transfer coefficient to be multiplied with the difference between T_{AST} and T_s .

$$H = \varepsilon\sigma\left(T_{AST}^i{}^2 + T_s^i{}^2\right)\left(T_{AST}^i + T_s^i\right) + h \quad \text{Eq. 17}$$

The section factor [10] gives a measure of how fast the steel can be heated as a high value indicates a slender section that is easier to heat quickly.

$$\frac{A_s}{V_s} = \frac{\text{Area of perimeter per unit length}}{\text{Volume of section per unit length}} \quad \text{Eq. 18}$$

The above calculations consider the body subjected to fire as a lumped heat body meaning that it will have uniform temperature.

3 Software

3.1 Introduction to CFD and FDS

FDS [2] is a Computational Fluid Dynamic, CFD, software developed by National Institute of Standards and Technology (NIST) [1]. The first version of the software was released in February 2000 and was made as an attempt to create a free, reliable software for fire simulations.

FDS is a finite difference model of fire driven gas flows. Finite difference method is a way to describe changes over time and space using Navier-Stokes equation in every prescribed point within the model space. Higher order derivatives renders more precise results but at an increasing computational cost. FDS is derived from differential equations up to the second order, which gives a satisfactory result.

Different CFD models use different techniques to solve the flow equations. In FDS the flow created is usually extremely transient and the most exact way to solve this would be the Direct Numerical Solution, DNS. DNS requires a very fine grid to be exact and much computational time. DNS is possible to use in FDS but only as an active choice.

Instead FDS as many other CFD models use a simulation technique where turbulence larger than grid size, containing the majority of the energy, is calculated with DNS. Turbulence smaller than grid size is on the other hand approximately modelled using a separate subgrid model. This technique is called Large Eddy Simulation and is an approximation of the “real” conditions in the simulation.

When calculating thermal radiation one needs to calculate the contribution from the complete spectrum in the fire. This is extremely time consuming and FDS assumes that the most important contributor to the thermal radiation is the soot. The thermal radiation is therefore seen as grey body radiation from the soot. This simplifies calculation since different wavelengths are not considered.

In comparing radiation experiments made by NIST and FDS simulations the conclusion was made in the FDS Technical Reference Guide [11] that a fair representation of radiation could be presented by the use of six spectral bands in the model. Meaning that instead of the radiation seen as an integrated value over the entire body it is seen as the sum of the integrated radiation from six different spectral bands. For special cases it is possible to force FDS to use nine spectral bands. This can give more accuracy in a model and accentuate different spectral bands that are considered important in a given model. In some cases where no radiation is needed for simulation purposes it can be turned off saving much simulation time.

The feature used to obtain output data is the measure device, or MD. This is a device set up by the user in the volume with specified orientation. The MD can be regarded as a point and does not affect the actual simulation in a way that could be the case in experiments.

To compare grid cell sizes from different set up, FDS User's Guide recommends the use of the quantity in Eq. 19 referring to the dimensionless diameter of the fire and element size in the mesh.

$$\frac{D^*}{\delta x}$$

Eq. 19

$$D^* = \left(\frac{\dot{Q}}{\rho_\infty c_p T_\infty \sqrt{g}} \right)^{\frac{2}{5}} \quad \text{Eq. 20}$$

3.2 Introduction to FEM and TASEF

The Finite Element Method (FEM) is a way to numerically solve analytical problems [12]. It is based on matrices and is very adaptable to solving temperature problems in elements exposed to fire. To solve temperature distribution over time numerically one needs to solve the heat balance equation

$$\bar{\mathbf{Q}} = \bar{\mathbf{K}}\bar{\mathbf{T}} + \bar{\mathbf{C}}\dot{\bar{\mathbf{T}}} \quad \text{Eq. 21}$$

Where $\bar{\mathbf{K}}$ is derived from the local thermal conductivity matrices given as

$$\bar{\mathbf{k}}^e = \frac{kA}{L} \begin{bmatrix} 1 & -1 \\ -1 & 1 \end{bmatrix}$$

and $\bar{\mathbf{C}}$ is derived from the local heat capacity matrices given as

$$\bar{\mathbf{c}}^e = \frac{ALc\rho}{2} \begin{bmatrix} 1 & 0 \\ 0 & 1 \end{bmatrix}$$

The method for calculating the time derivative of the node temperature, $\dot{\bar{\mathbf{T}}}$, is given on the form $\dot{\bar{\mathbf{T}}} = (\bar{\mathbf{T}}^{j+1} - \bar{\mathbf{T}}^j)/\Delta t$ where $\bar{\mathbf{T}}^j$ is the node temperature vector at time step j and Δt is a chosen time increment.

This gives the equation

$$\bar{\mathbf{Q}} = \bar{\mathbf{K}}\bar{\mathbf{T}}^{j+1} + \bar{\mathbf{C}}(\bar{\mathbf{T}}^{j+1} - \bar{\mathbf{T}}^j)/\Delta t \quad \text{Eq. 22}$$

with the implicit solution

$$\bar{\mathbf{T}}^{j+1} = (\bar{\mathbf{C}}/\Delta t + \bar{\mathbf{K}})^{-1} \bar{\mathbf{Q}}^j + \bar{\mathbf{C}}\bar{\mathbf{T}}^j/\Delta t \quad \text{Eq. 23}$$

It is important to note that the time increment can cause instability in the calculations if it exceeds the critical time increment for any given element (see Eq. 24).

$$\Delta t_{cr} \approx \frac{c\rho}{k}(\Delta x)^2 \quad \text{Eq. 24}$$

TASEF [13] is a software that can solve Eq. 21 in different ways. The main method that will be used in this thesis is to calculate Q as a function of a prescribed fire temperature. The software was developed by Ulf Wickström as a tool to calculate temperature distributions under prescribed conditions. The program is developed for use on two dimensional and axisymmetrical elements.

The basic equation solved by finite element method in TASEF presented in the User's Manual [14] is the transient, two-dimensional heat transfer equation.

$$\frac{\partial}{\partial x} \left(k \frac{\partial T}{\partial x} \right) + \frac{\partial}{\partial y} \left(k \frac{\partial T}{\partial y} \right) - \frac{\partial e}{\partial t} + Q = 0 \quad \text{Eq. 25}$$

This equation describes the heat flux in two dimensions with account to the specific enthalpy, e , and internally generated heat, Q .

The body to be analysed is divided into elements of appropriate size. Both rectangular and right angular triangular shapes are possible to create with the

input program INTASEF. Elements in TASEF are assigned material properties via INTASEF. If specified in INTASEF, TASEF consider thermal properties varying with temperature and latent heat due to evaporation of water. The critical time increments presented in Eq. 24 are calculated in TASEF and the nodal temperatures at given time steps are then approximated over the body.

In heat transfer calculations based on prescribed temperature TASEF uses Eq. 11 or Eq. 12. Eq. 11 is solved specifying T_r and T_g separately and Eq. 12 with the use of one single fire temperature.

TASEF allows the user to specify ε , σ , h and n in Eq. 11 and Eq. 12 depending on assumed local conditions. The user's manual gives $\varepsilon = 0.8$, $\sigma = 5.67 \cdot 10^{-8} \text{ W/m}^2\text{K}^4$, $h = 25 \text{ W/m}^2\text{K}$ and $n = 1$ as good reference values.

Properly used, TASEF gives good results and finer mesh gives more exact results [15]. As is the problem for most calculation software a lot depends on the input given. Today there are four possible methods for temperature input.

1. ISO 834 or EN 1363-1
2. Eurocode Parametric fires
3. Constant gas temperature
4. Specified time – temperature curve based on temperature input from the user at given time.

In the use of AST the temperature input is made with method four.

4 Results

4.1 Verification of AST with spread sheet calculations via the verification of steel temperature calculated in FDS

To verify the use of AST as a possible method for calculating heat transfers in steel it is necessary to verify the wall temperature given in FDS. The method for verification of the wall temperature given in FDS is set up as a small room illustrated in Figure 4-1. The geometry is cubical with the side of 1.0 meter. The floor with a temperature of 800 °C and ambient temperature set to 20 °C.

The body subjected to testing is the ceiling. It is set up as a steel plate of 0.01 m thickness in order to be regarded in temperature calculations as lumped. This facilitates the comparison with the uniform temperature from spread sheet calculations since the surface temperature from FDS can be assumed to represent the temperature of the entire body.

To obtain a result easy to predict and understand it was important to avoid the influence of unnecessary energy loss, hence in the box all walls were made adiabatic. The grid cell size used in this simulation was 15.625 cm³ or cubes with the side of 2.5 cm.

Measure devices or MD's (see chapter 3.1) were placed 0.2 m apart covering the ceiling with corresponding measure devices 0.1 m below for measure of gas temperature (see Figure 4-1).

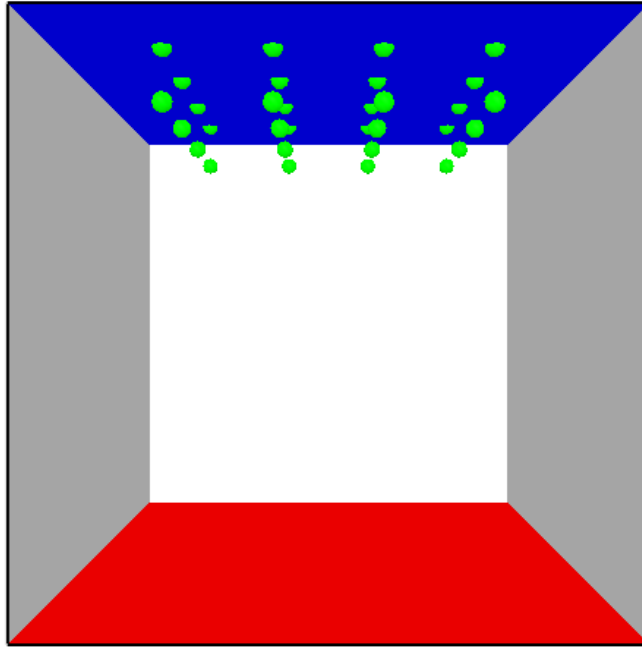


Figure 4-1 Setup of the cube with the side of 1.0 meter.

The output from MD's needed for this verification was:

- WALL_TEMPERATURE (T_w)
- ADIABATIC_SURFACE_TEMPERATURE (T_{AST})
- RADIATIVE_FLUX
- CONVECTIVE_FLUX

With data from the four reference points in the centre of the ceiling a mean value is calculated. Eq. 26 and Eq. 27 are used to calculate backwards the values of T_r and T_g (see chapter 2.1 for reference) from the given wall temperature and heat fluxes calculated by FDS. ε , h and n are assumed in this chapter to be constant values at 0.8, 25 W/m²K and 1 respectively.

$$T_r = \sqrt[4]{\frac{\dot{q}_{rad}''}{\varepsilon\sigma} + T_w^4}$$

Eq. 26

$$T_g = \frac{\dot{q}_{con}''}{h} + T_w$$

Eq. 27

The result of the calculations over a simulation time of 40 min is presented in Figure 4-2.

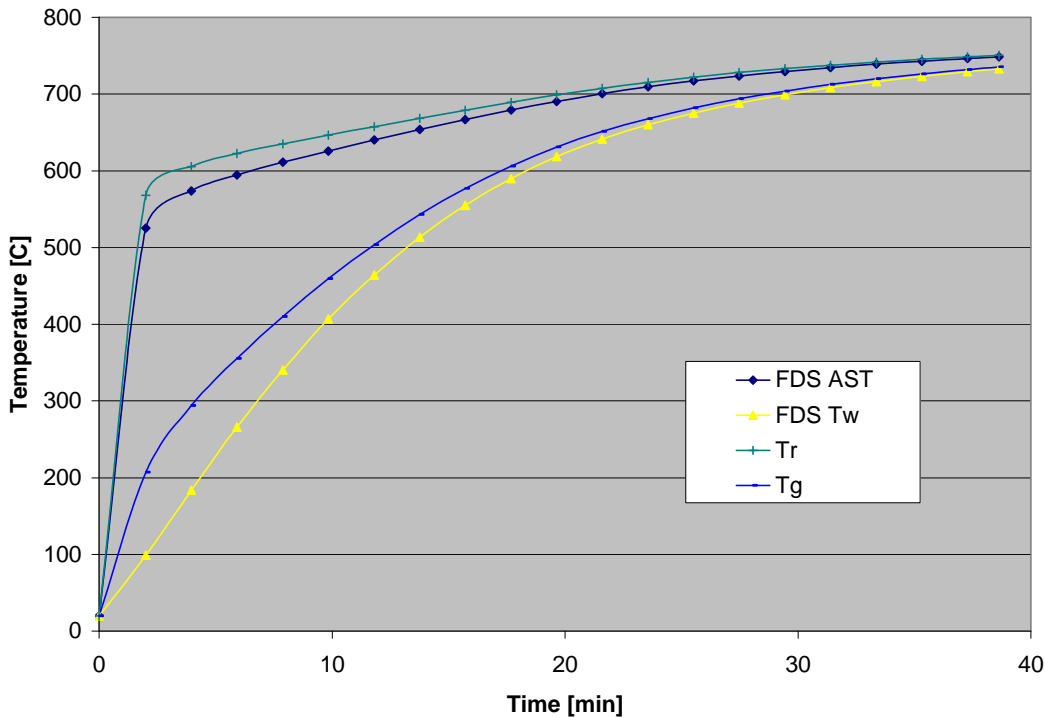


Figure 4-2 T_{AST} , T_g and T_w from FDS simulation and T_r and T_g calculated from Eq. 26 and Eq. 27.

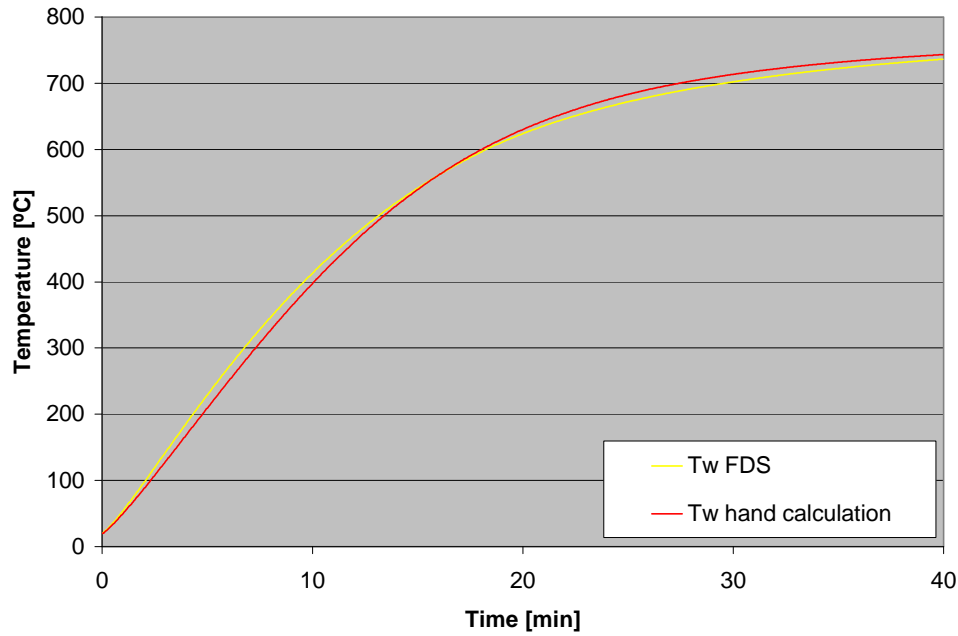
Figure 4-2 shows, as explained in chapter 2.3, that T_{AST} assumes a value between T_r and T_g closer to T_r . Comparing the wall or actually the ceiling temperature directly from the FDS simulation with the corresponding temperature from spread calculations via T_{AST} should give the same result.

In chapter 2.1.2 it is explained how h is calculated analytically. This method is also used in FDS. Since FDS calculates the convection coefficient, h , analytically, the value can vary over time. It is therefore difficult to compare the convection from FDS with the convection from spread sheet calculation with an

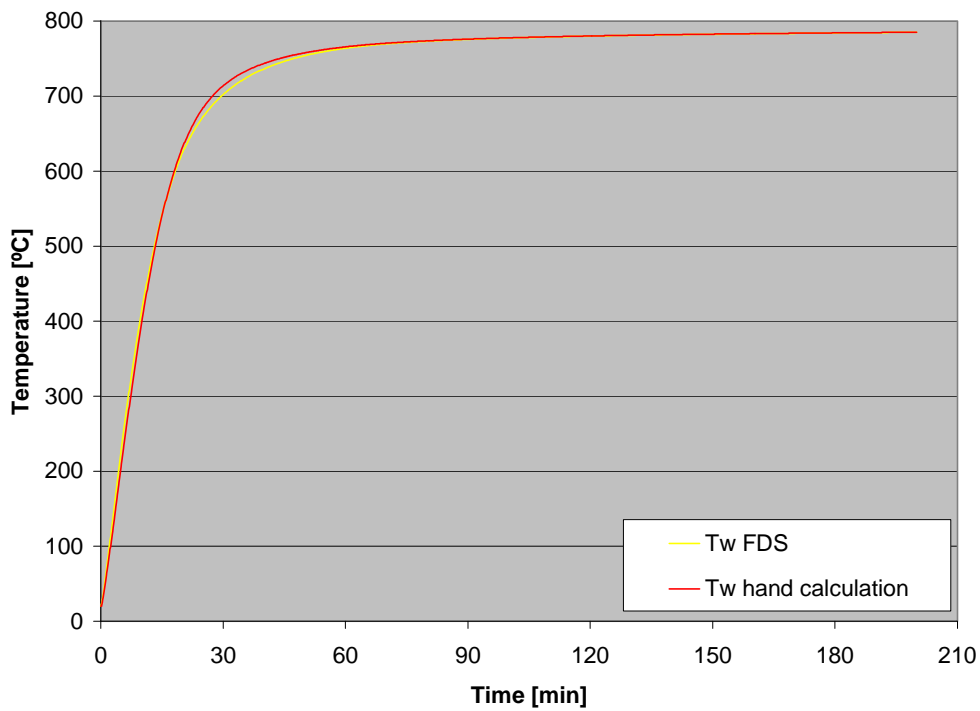
assumed constant value. This can explain the result in Figure 4-3a where spreadsheet calculations based on Eq. 17 and T_{AST} only agrees almost perfectly with the wall temperature calculated in FDS.

An explanation can be that the steel reacts slower early in the simulation and as the simulation progresses, extremely turbulent conditions with high velocities are created. In Eq. 9 and Eq. 10 the velocity of the flowing media, in this case the heated gas is an important factor. The high velocities in the later stage give a convection coefficient higher than $25 \text{ W/m}^2\text{K}$ in FDS.

Seen over a longer period of time the wall temperature should approach $800 \text{ }^\circ\text{C}$. The simulation shown in Figure 4-3b, made over a period of 200 minutes indicates that the assumption is correct.



a) Simulation over 40 min



b) Simulation over 200 minutes showing the wall temperature slowly approach 800 °C.

Figure 4-3 Ceiling temperatures calculated directly in FDS simulation and the corresponding temperature, calculated with the method presented in chapter 2.4.

4.2 Calculation of beam temperature with TASEF

The latest version of TASEF has a multifire function allowing the user to specify different fire conditions to different boundary groups. This gives the opportunity to input experimental or simulated data as boundary conditions to the two dimensional cross section of a beam. One input method in TASEF is to use T_f as the calculation temperature which as shown in this report corresponds to the adiabatic surface temperature, T_{AST} .

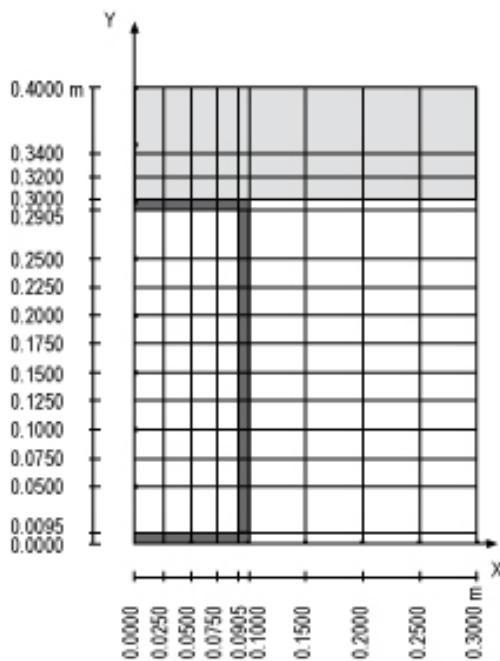


Figure 4-4 Geometry of model created in TASEF (for file see Appendix A).

The TASEF model shown in Figure 4-4 has the dimensions of 300 mm x 200 mm and a thickness of 9.5 mm corresponding to a simplified version of the dimensions on a beam of model RHS300. The same dimensions are used in FDS. Some assumptions were made to simplify the calculations:

- The simulation is symmetric around the y – axis.
- Nodes in the steel section close to each other are coupled to save computational time.
- Heat exchanged by radiation and convection between the interior surfaces of the hollow beam section is considered.

- All surfaces have the emission coefficient of 0.8.
- All surfaces have the convection coefficient of $h = 25 \text{ W/m}^2\text{K}$

The room in which the simulations are run is a cube (see Figure 4-5) of dimensions 1.6 x 1.6 x 1.6 m with a door on one side with dimensions 0.4 m x 1.2 m. The sets of reference points located at a certain distance from the inner wall are referred to as reference sets. These sets are located along the beam at the distance of 0.1, 0.8 and 1.5 m from the inner wall (see Figure 4-6) and are referred to as reference set 1, 2 and 3 respectively. The cross section locations of reference points are shown in Figure 4-7. The energy source is located at the centre by the inner wall with a heat release of 500 kW and the dimensions of 0.2 m x 0.2 m. Grid cells with the side of 2.5 cm are used in the model.

In the scenario with a smaller beam (200 mm x 100 mm with thickness of 15 mm) the reference point set up is made relative, i.e. reference point b is for example still located on the middle of the side and not on a fixed distance from the ceiling compared to the simulations with a larger beam. The same is for reference points d and e which are located 10 cm from the side of the beam and not on a fixed distance from the symmetry line.

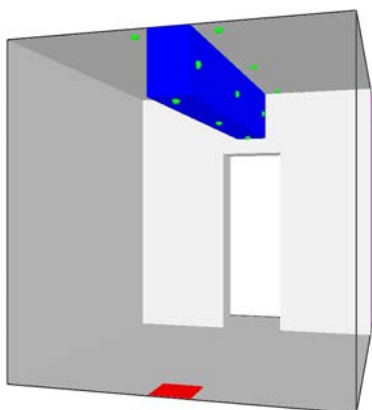


Figure 4-5 The modelled room in which the different scenarios were simulated.

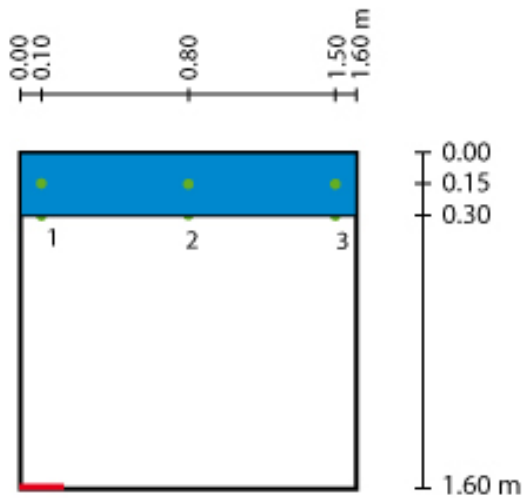


Figure 4-6 Dimensions of the cube seen from the side and location of reference sets 1, 2 and 3 (green dots). Red rectangle represents the energy source and blue rectangle the beam.

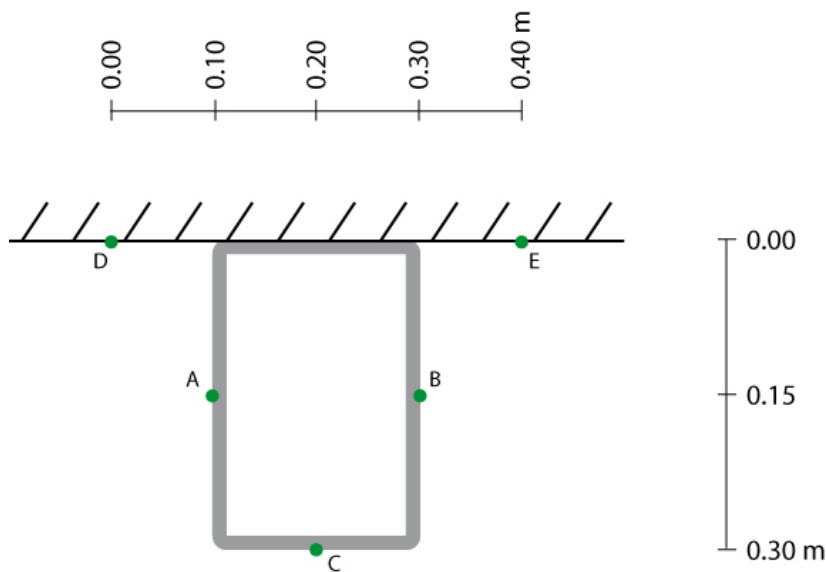


Figure 4-7 Set up of reference points seen as a cross section of the beam.

The steel temperature calculated in FDS is compared to the steel temperature calculated in TASEF with AST from reference point b, c and e in the FDS model. Eq 14 is then used to calculate the heat transfer from the fire to the steel section.

The results from reference point 1b and 1c are seen in Figure 4-8. The temperature obtained by the 2-D TASEF model is lower than the temperature

obtained directly from FDS as the heat transfer calculations in FDS are made only in one dimension. Hence FDS is not considering the loss of heat by conduction in the steel or the exchange of heat by radiation and convection between the enclosure void surfaces.

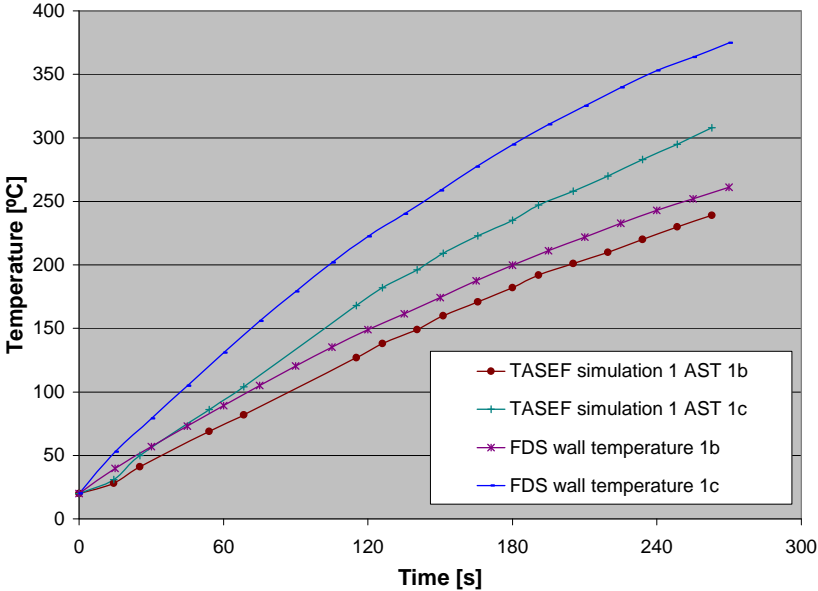


Figure 4-8 Beam temperature in reference point 1b and 1c from FDS directly and from calculations in TASEF using Eq. 14 with T_{AST} as boundary condition.

In reference points 2b and c (see Figure 4-9) the deviations are small.

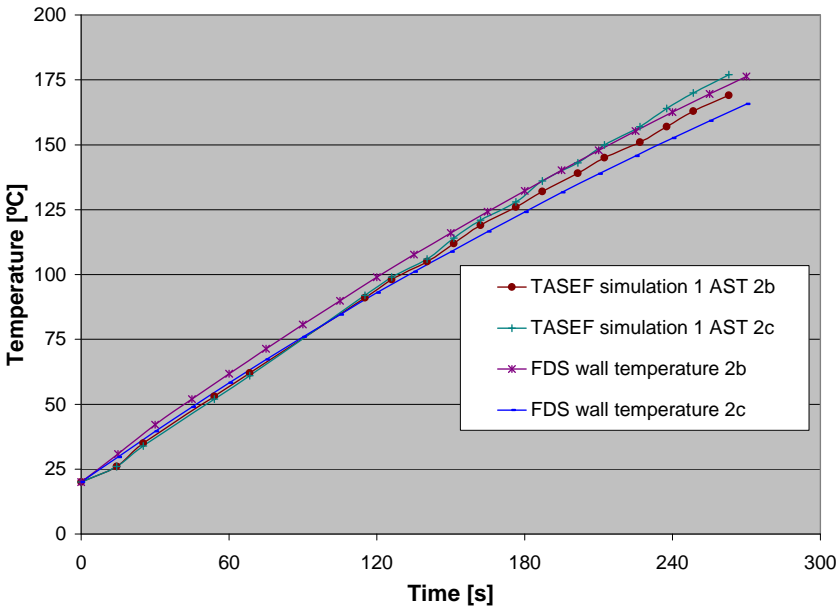


Figure 4-9 Beam temperatures in reference point 2b and 2c from FDS directly and from calculations in TASEF using Eq. 14 with T_{AST} as boundary condition.

4.3 Verification of the use of AST in heat transfer calculations

The third step in this thesis is to try to verify the theory of the AST being able to create a replica of the fire conditions in a critical area regardless of beam dimensions. To test this, six different scenarios were simulated (see Table 1) using the set up from chapter 4.2. If the theory is correct, the values of T_{AST} from one simulation could be used on different beams as long as the fire scenario is the same.

Table 1 Experiment set up for test of the AST as a good method of transferring fire temperature to a beam

	Location of heat source (See Figure 4-10)	Effect of heat source	Beam dimensions [mm]
Simulation 1	1	500 kW	300 x 200 thickness: 9.5
Simulation 2	1	500 kW	200 x 100 thickness: 10.5
Simulation 3	2	500 kW	300 x 200 thickness: 9.5
Simulation 4	1	500 kW	Only Plate Thermometers
Simulation 5	1	100 kW	300 x 200 thickness: 9.5
Simulation 6	1	100 kW	200 x 100 thickness: 10.5

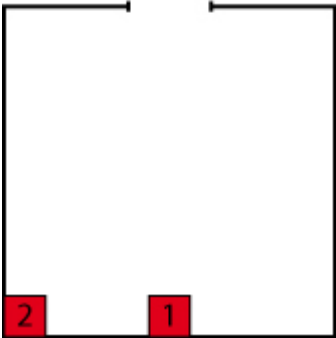


Figure 4-10 Location of heat source 1 and 2 in the modelled room. The upper end of the figure showing the opening.

Four comparisons are made to test the assumption that T_{AST} could give a good input value from a fire scenario regardless of beam set up. The adiabatic surface temperature is calculated in reference point b, c and e in every reference set. The calculated temperature from reference point e is only used as input to TASEF. The assumption is made that the value $h = 25 \text{ W/m}^2\text{K}$ could be used for TASEF temperature calculations in all scenarios.

The first comparison is made to see if T_{AST} from simulation 1 and 2, same heat source but different beams, have any agreement. The prediction of the result would be that the temperature calculated in reference point c on the smaller beam should be lower as the surface, from which the calculated values are taken, is located higher and therefore not engulfed in flames as much as the larger beam. Calculations in reference point b, on the side should show only small deviation. In the reference points further away from the energy source the deviation is assumed to be none or very small as conditions are more stable. If so, the theory would work. The results from this comparison are presented in Figure 4-11, Figure 4-12 and Figure 4-13.

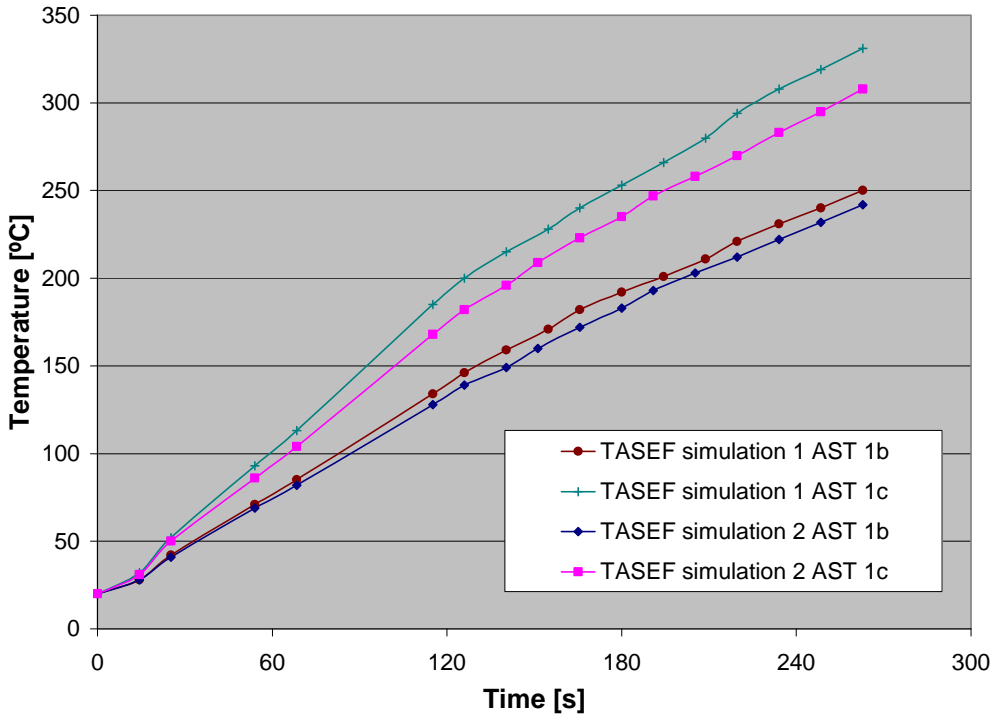


Figure 4-11 Beam temperature in reference point 1b and 1c calculated on the beam in simulation 1 with the use of AST from simulation 1 and 2 separately.

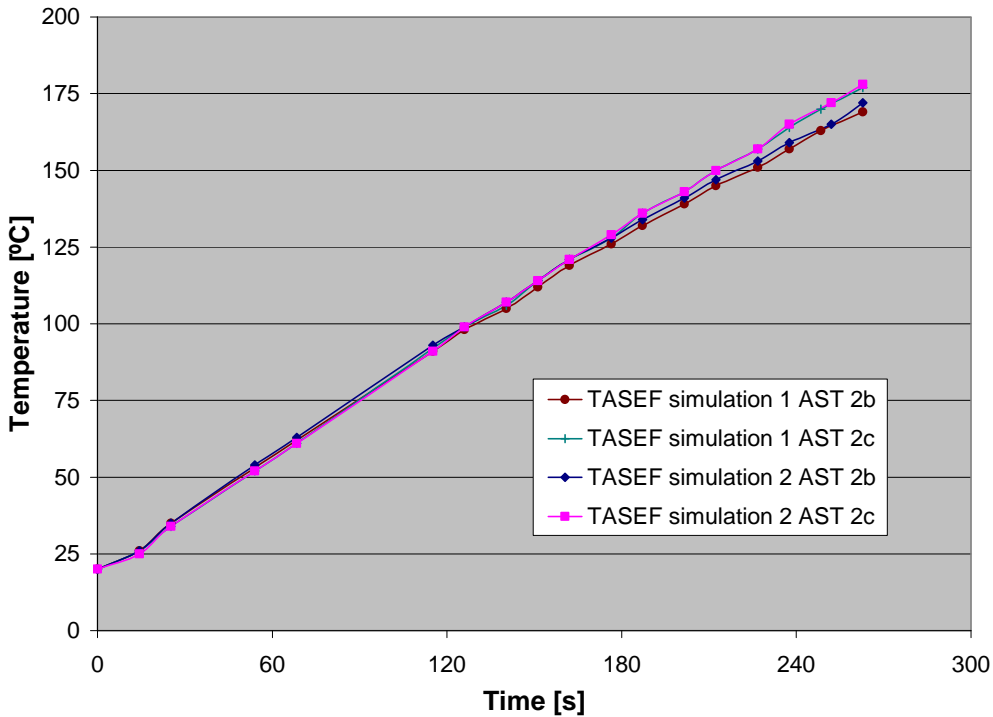


Figure 4-12 Beam temperature in reference point 2b and 2c calculated on the beam in simulation 1 with the use of AST from simulation 1 and 2 separately.

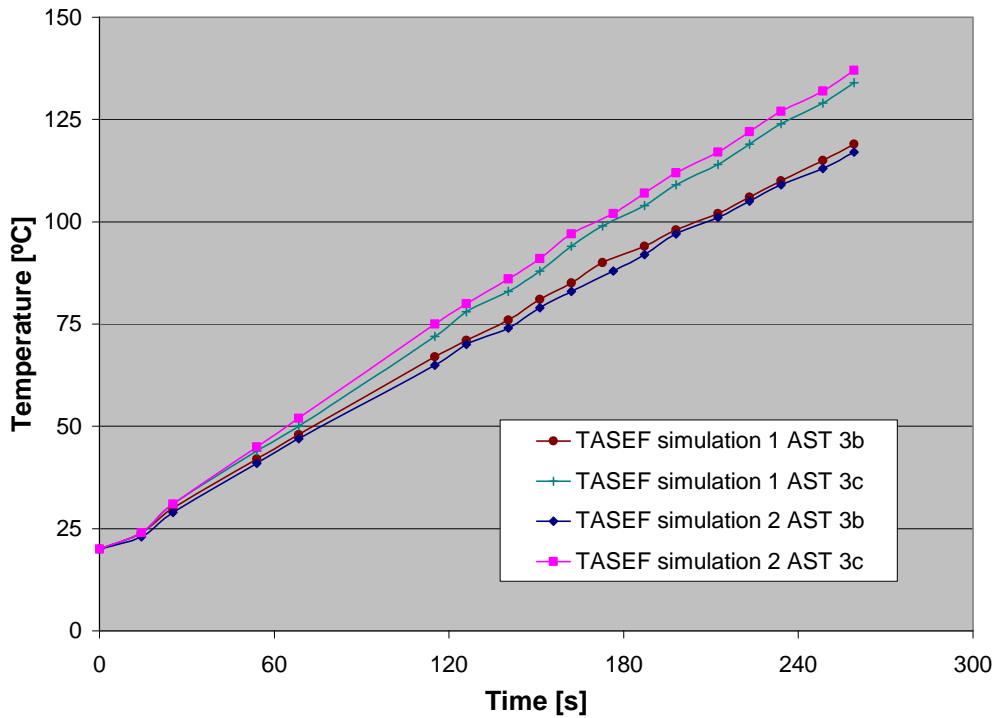


Figure 4-13 Beam temperature in reference point 3b and 3c calculated on the beam in simulation 1 with the use of AST from simulation 1 and 2 separately.

The second comparison is made between simulation 1 and 3 to see if an extension of the theory is possible with regards to the location of the energy source. This comparison is made with the same beam but different location of the energy source (see Table 1). In this T_{AST} will be different in reference point a and b in simulation 3 and a non symmetric model had to be made in TASEF. This model is similar to the one seen in Figure 4-4 with same dimensions only twice as big thus giving different results from reference points a and b. The temperature calculations (see Figure 4-14) should deviate largely on the sides with higher temperature in reference point b as it is the reference point facing the energy source. This comparison is made to see how large the deviation is between the simulations and is therefore only made at reference set 2.

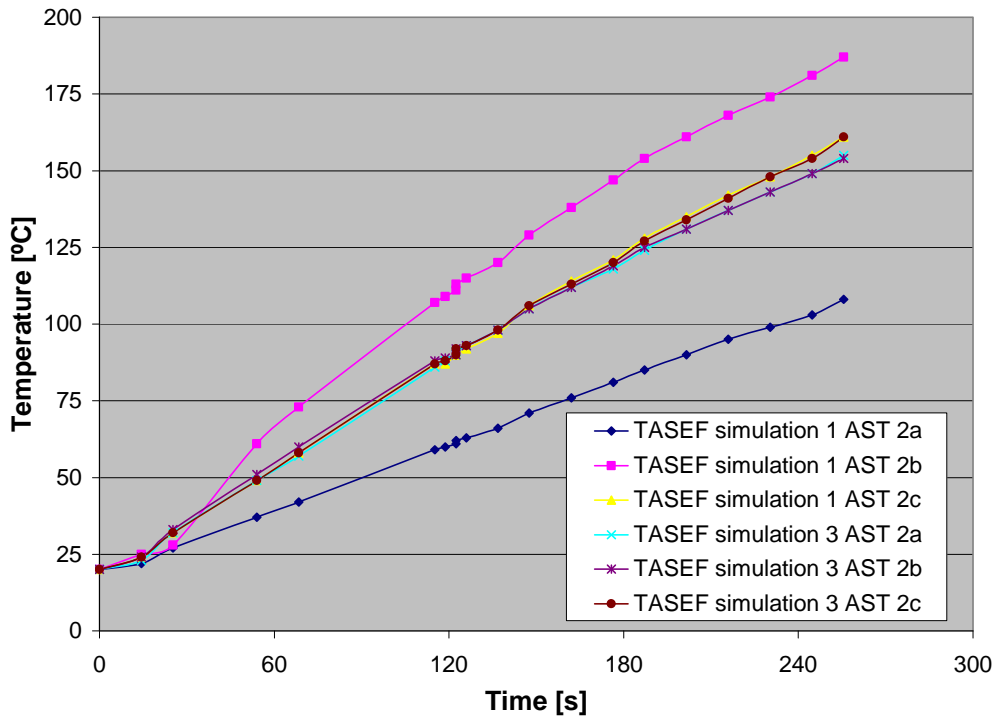


Figure 4-14 Beam temperature in reference point 2b and 2c calculated on the beam in simulation 1 with the use of AST from simulation 1 and 3 separately.

An interesting thing to notice here is that the average overall temperature in the beam is the same even if the sides differ a lot. The calculated temperature in reference point c is almost identical.

The third comparison with only Plate Thermometers (see Figure 4-15) versus beam is made in simulation 1 and 4 to see if it is possible to run the simulation without beam in the set up. The Plate Thermometers in this set up is located 0.1 m outside the surface to which it is supposed to be compared. The location should only have a minor effect since values from different sized beams should be comparable.

The simulation without beam creates different conditions in aspects such as shadow effect and turbulence. Therefore the result (see Figure 4-16, Figure 4-17 and Figure 4-18) is supposed to deviate although not as much as the previous comparison. This comparison should give better agreement in a larger test

volume, with the beam further from the energy source, where turbulence and radiation is not affected as much by the being of one beam.

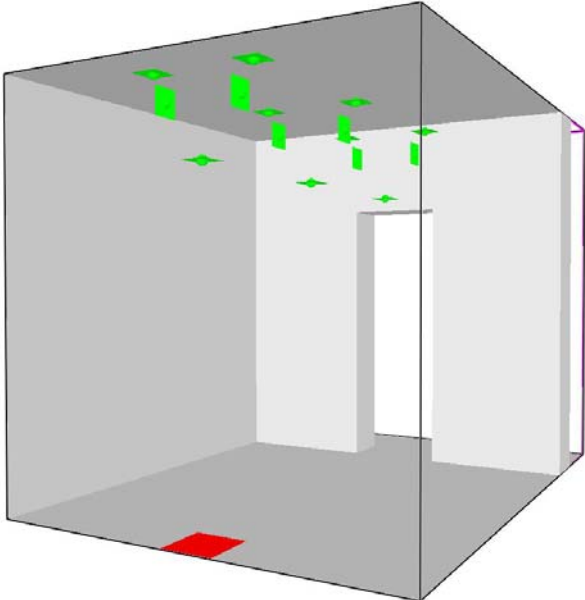


Figure 4-15 Set up of model only with Plate Thermometers and no beam.

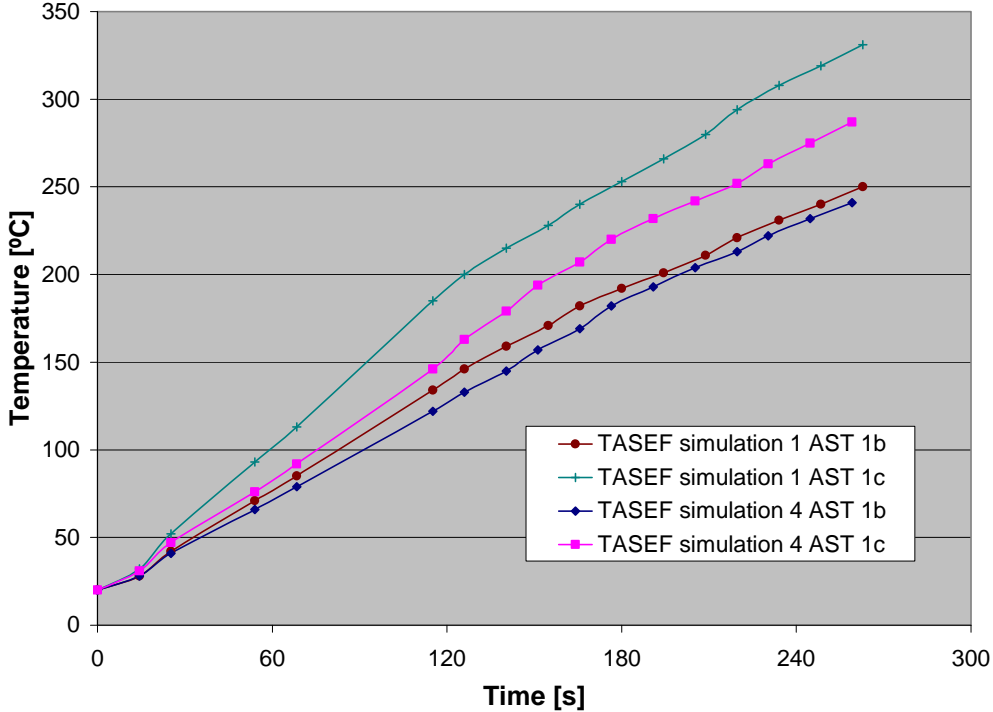


Figure 4-16 Beam temperature in reference point 1b and 1c calculated on the beam in simulation 1 with the use of AST from simulation 1 and 4 separately.

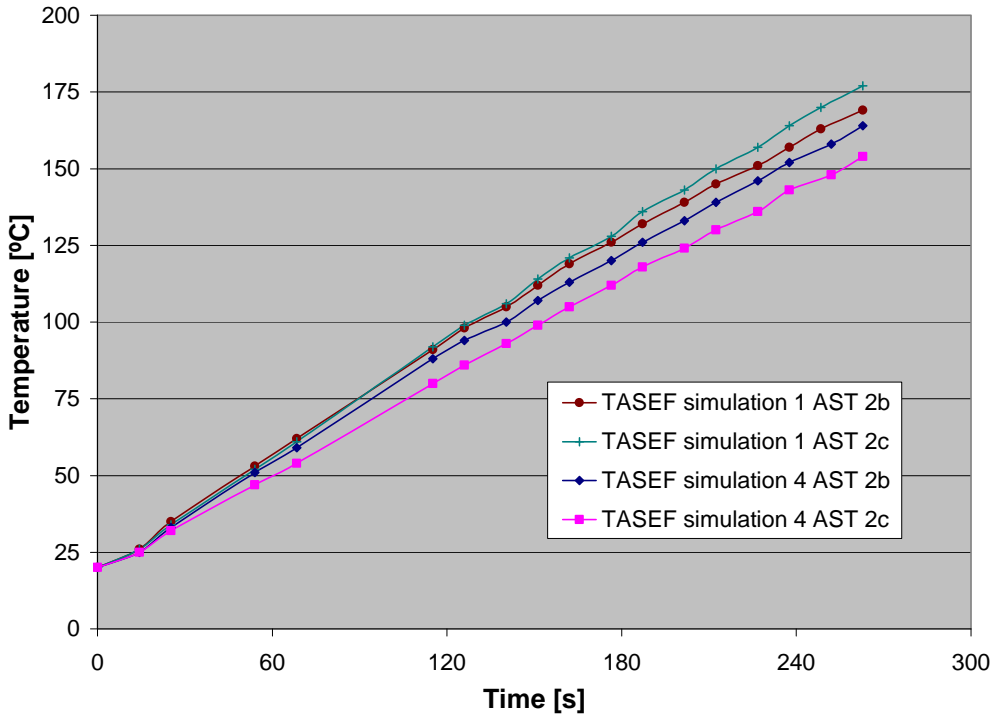


Figure 4-17 Beam temperature in reference point 2b and 2c calculated on the beam in simulation 1 with the use of AST from simulation 1 and 4 separately.

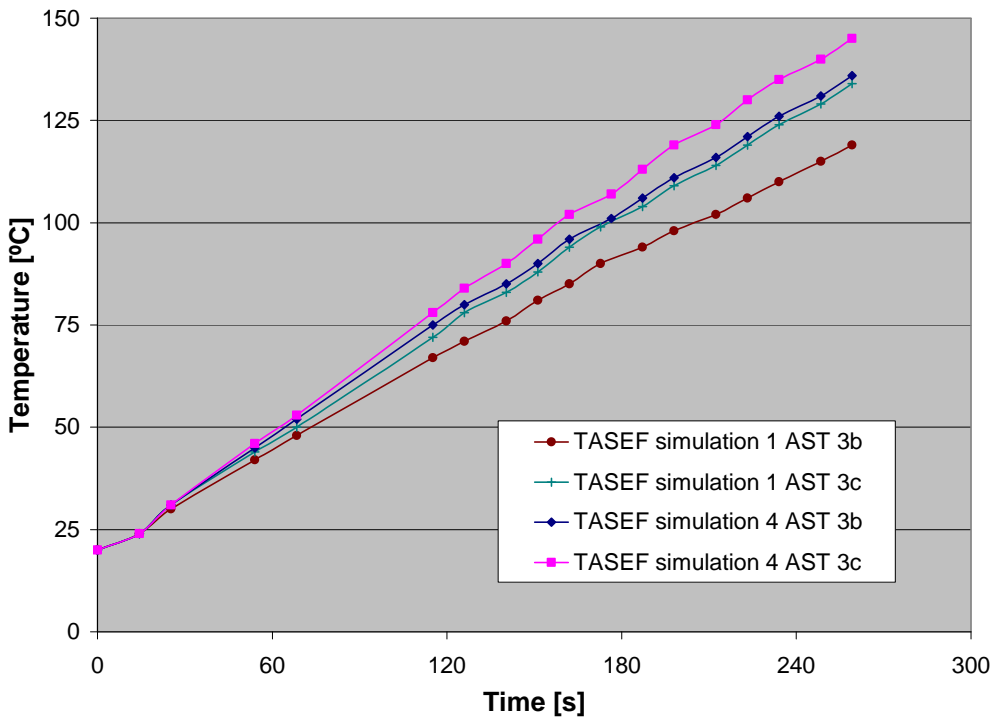


Figure 4-18 Beam temperature in reference point 3b and 3c calculated on the beam in simulation 1 with the use of AST from simulation 1 and 4 separately.

The fourth comparison was made between simulation 5 and 6 to see if similar results would be obtained as in the first comparison with a different effect on the heat source. This should give a better agreement than in the first comparison since the flame height is lower and conditions surrounding the beam more stable. The result is presented in Figure 4-19, Figure 4-20 and Figure 4-21.

In Figure 4-19 it is possible to see a deviation that is larger than expected. This can be explained with the flame height. The height of the flames in this experiment is in the region of 1.2 to 1.4 m above the energy source engulfing measure point 1c on the larger beam more often than the corresponding point on the smaller beam. The temperature in the flames is considerably higher than the temperature just above giving a higher value of T_{AST} in simulation 5 with the larger beam.

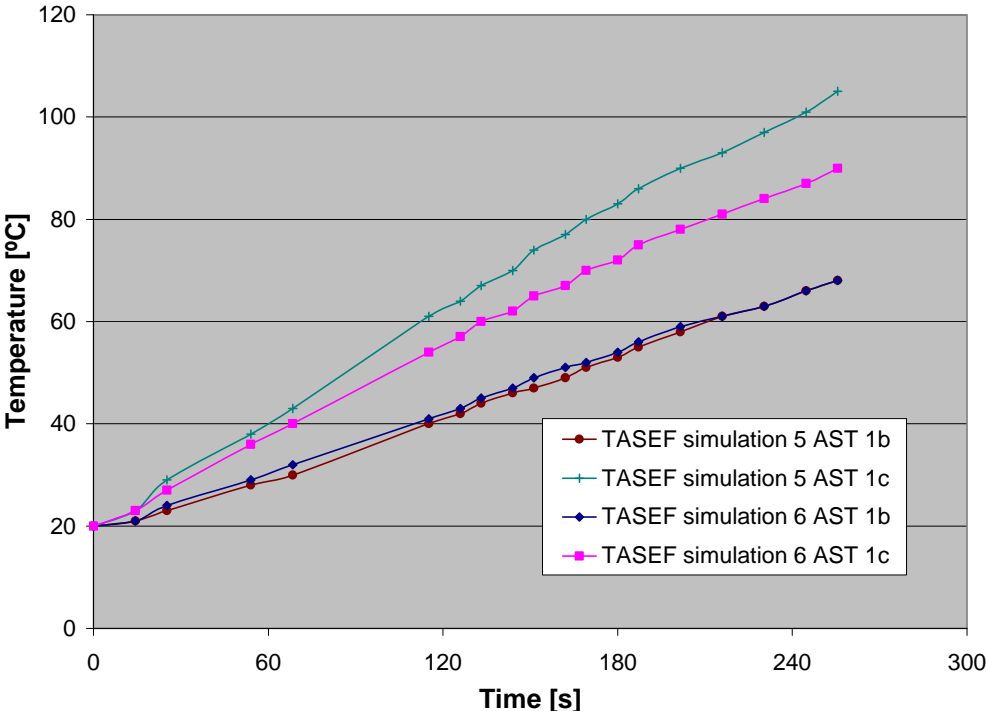


Figure 4-19 Beam temperature in reference point 1b and 1c calculated on the beam in simulation 2 with the use of AST from simulation 2 and 6 separately.

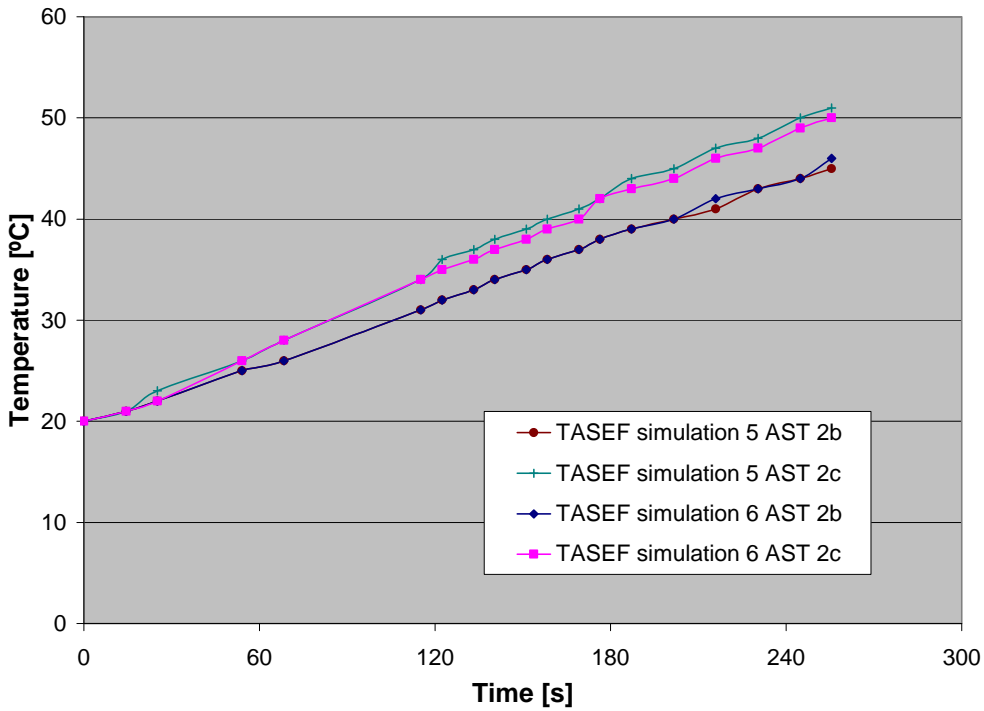


Figure 4-20 Beam temperature in reference point 2b and 2c calculated on the beam in simulation 2 with the use of AST from simulation 2 and 6 separately.

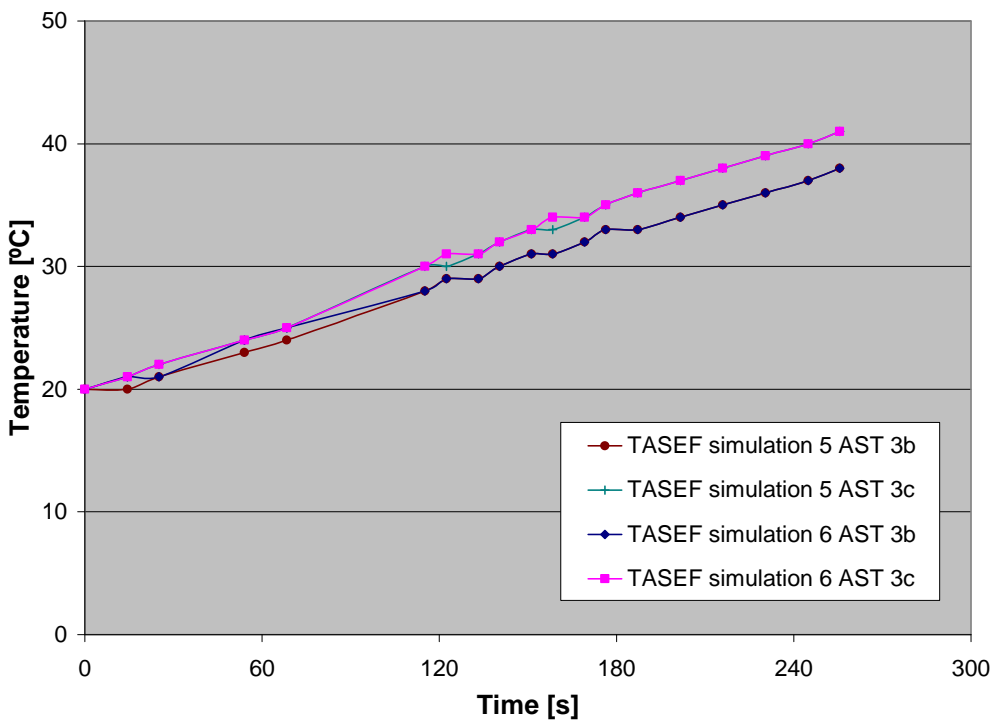


Figure 4-21 Beam temperature in reference point 3b and 3c calculated on the beam in simulation 2 with the use of AST from simulation 2 and 6 separately.

4.4 Setup of a fire scenario that can be experimentally verified

4.4.1 Geometry of experiments

The test volume in the sensitivity analysis is made as one of SP's furnaces with the dimensions 3 m x 5 m x 2.5 m with an opening of 2 m x 1.2 m on one wall. The energy source is modelled as a plate with dimensions of 0.2 m x 0.2 m and the constant effect of 500 kW. The plate is located on the centre line of the test volume close to the inner wall (see Figure 4-22).

The sensitivity analysis is made with two different beam set ups, one symmetric and one asymmetric as seen in Figure 4-22. The asymmetric beam is placed with the outer side of the beam one meter from one of the sidewalls in the furnace.

The experiments are performed with a model of the structural hollow section RHS300. The dimensions of the RHS300 is 304.8 mm x 203.2 mm and a thickness of 9.5 mm. This is then simplified to adapt to the grid in FDS to a beam of dimensions 300 mm x 200 mm, the thickness still 9.5 mm.

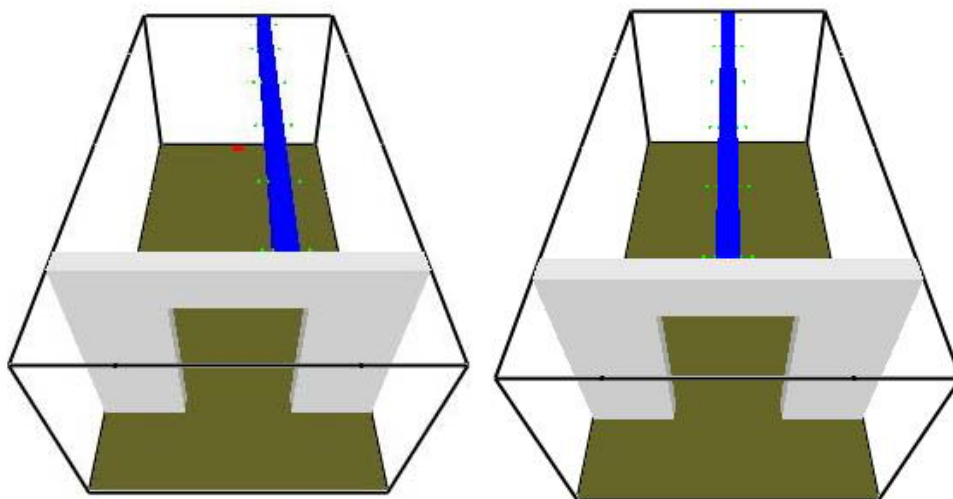


Figure 4-22 Asymmetric and symmetric set up of beam rendered in FDS. Red plate represents energy source (hidden behind beam in the symmetric case). Green dots represent reference points with measure devices.

Six sets of reference points are located along the beam (see Figure 4-22). These reference sets are located, starting over the energy source, at the distances of 0.1, 1.0, 2.0, 3.0, 4.0 and 4.9 m from the inner wall. The numbering of the reference point sets starts with number 6 directly over the fire (or 0.1 m from the inner wall) and continues down to 1 (4.9 m from the inner wall). The set up of reference points in each set on the beam are shown in Figure 4-23 over a cross section of the beam.

To assure values that are comparable between simulations with different grid sizes it is assumed that the reference points have to be located in a node common for all grid sizes. Since the simulations with the coarsest grid have grid cells with sides of length 0.1 m the reference point has to be located at a distance that is a multiple of 0.1 from the ceiling. Reference point a and b are therefore located 0.1 m from the ceiling and not on the centre of the side at 0.15 m from the ceiling. A list of the measures devices used in each of the reference points is given in Table 2.

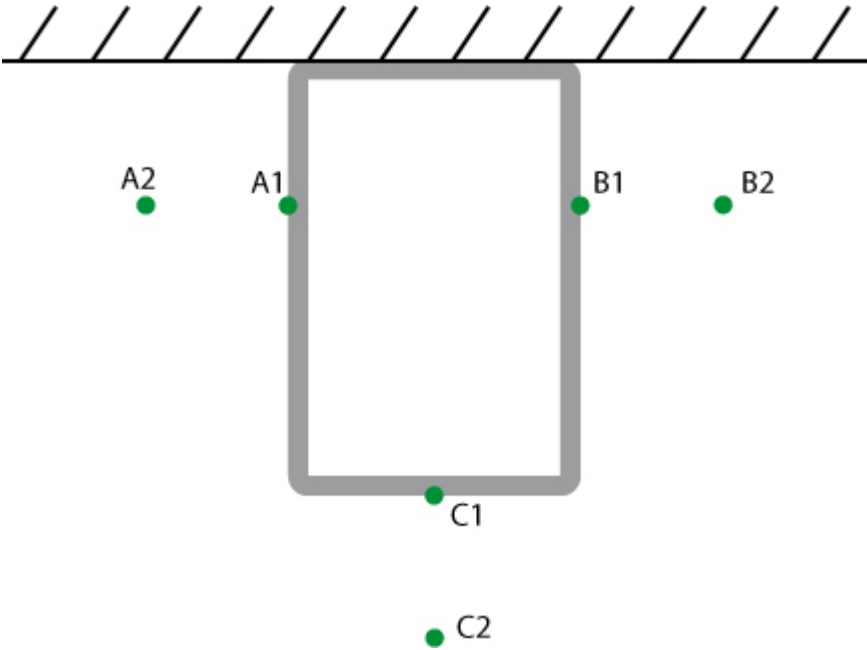


Figure 4-23 Cross section of beam showing location of MD's.

Table 2 Location of MD's in Figure 4-23

	A1	A2	B1	B2	C1	C2
Adiabatic Surface Temperature	X		X		X	
Wall Temperature	X		X		X	
Heat Flux	X		X		X	
Gas Temperature		X		X		X
Gas Velocity		X		X		X

4.4.2 Set up of FDS model

To decide what grid size dimension to use in the experimentally verifiable model there are some factors to be considered. The grid size has to be determined with the use of a sensitivity analysis, it has to be determined if the use of the mirror function embedded in FDS is possible to use and finally if the values calculated in a secondary mesh of different grid size can be used.

4.4.2.1 Geometry

The geometry of the model is made to mimic the furnace at SP with an extra space outside the opening of the furnace. This way difficulties with boundary conditions are moved away from the opening thus not disturbing the simulation results in the simulated furnace.

The simulated furnace has concrete walls with a thickness of 0.2 m which is an attempt to assume semi infinity.

The asymmetric model is used to see the results from sensitivity analysis in a full scale scenario. This requires much time to compute and is therefore only made with three different grid sizes. Comparisons are made between the full scale and mirrored simulations in the symmetric case (see Figure 4-22 and Figure 4-24). If this works as intended it would reduce the simulated volume to half the size saving simulation time.

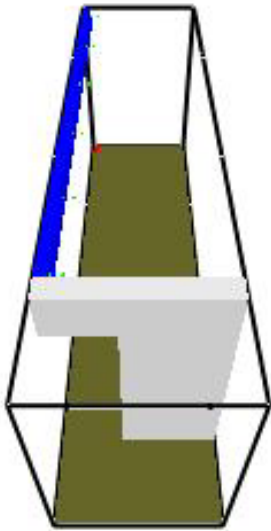


Figure 4-24 Mirrored symmetric set up the model.

4.4.2.2 Mesh

To save processing time the geometry is divided into two meshes (see Figure 4-25). And the sensitivity test is performed with different grid cell size in the primary mesh. The grid cell sizes used in the analysis are calculated as the dimensionless number presented in Eq. 20 and referred to as grid cell size A to E (see

Table 3). The secondary mesh is kept constant at grid cell size A while the grid cell size in the primary mesh is changed between the simulations.

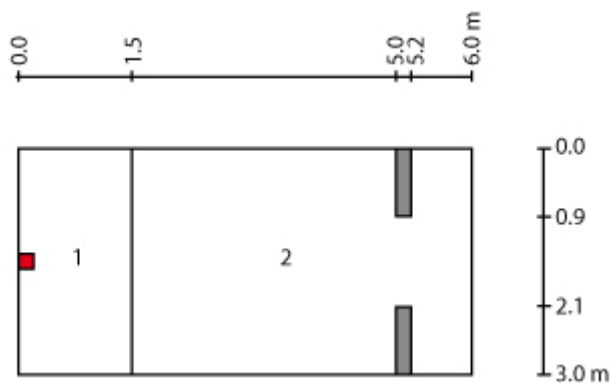


Figure 4-25 The primary (1) and secondary (2) mesh in the model made for the sensitivity analysis. The red square represents the energy source.

Table 3 Denomination of the different grid sizes used in this chapter.

Grid cell size [cm]	$\frac{D^*}{\delta x}$	Grid cell size referred to in text as:
10 x 10 x 10	7.27	Grid cell size A
5 x 5 x 5	14.54	Grid cell size B
3.3 x 3.3 x 3.3	21.81	Grid cell size C
2.5 x 2.5 x 2.5	29.08	Grid cell size D
2 x 2 x 2	36.35	Grid cell size E

The results from these simulations are predicted to converge as the grid cell size is refined. The first step is to compare the asymmetric full scale scenario with three different simulations of grid cell size A, B and D. The reference points used are reference points 5a, b and c since they are not directly above the energy source but still in the primary mesh. The reason to use the reference points not directly over the energy source is that the conditions are assumed to be more stable further away from the energy source and the flame.

This was made to be able to see if it was possible, in this early stage to see any convergence and also to see if T_{AST} from the different reference points in each reference set gives the predicted result. The prediction is that the temperature calculation in reference point 5a facing the energy source have a much higher T_{AST} than T_{AST} in reference point 5b (see Figure 4-26). The value used in the comparison is calculated with the output data from FDS as a mean value over 30 s.

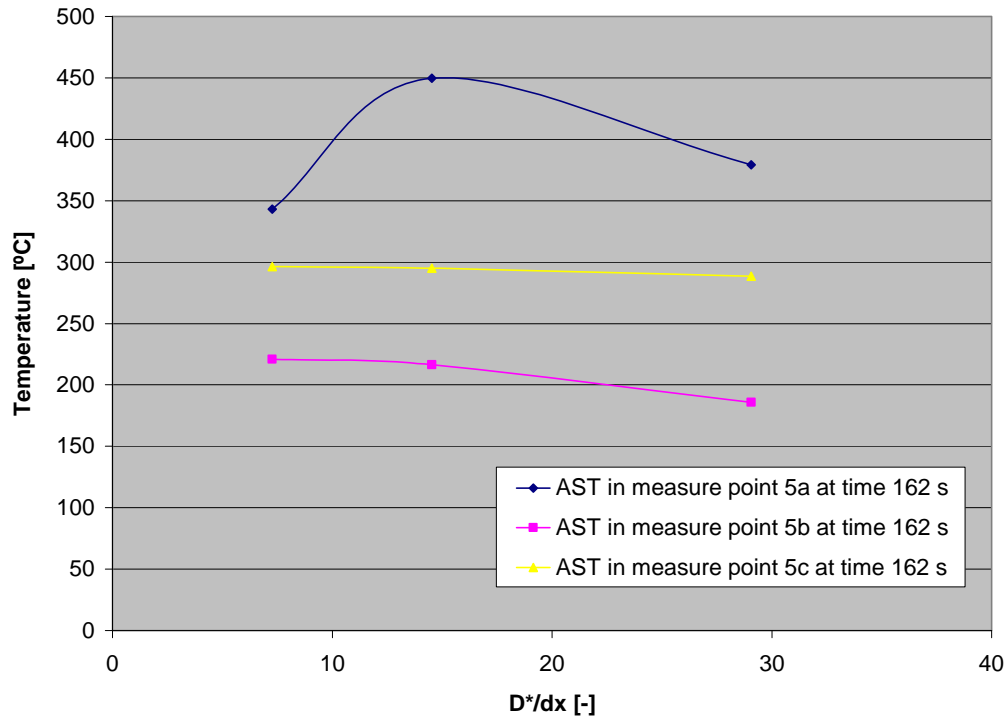


Figure 4-26 T_{AST} with grid cell size A, B and D calculated at reference set 5 in the asymmetric model at time 162 s.

As can be seen the prediction of T_{AST} works but there is a lack of convergence in the results. Hence no conclusion can be made from these simulations and further simulations are needed. The same tendency of no convergence could be seen in the simulations with the symmetric mirrored and the more detailed analysis are therefore made in that scenario to save processing time.

The results calculated in reference point 5b and 5c in the mirrored symmetric study is shown as mean values over 30 s in Figure 4-27. Since all values from grid cell size A to D indicates the same tendencies regardless of time interval it is assumed that further simulations over shorter simulation times would be possible. This regarded that the comparison is made with the other calculations at the same time interval. Hence grid size E was simulated during 90 seconds giving a mean value at 75 s. Figure 4-28 shows convergence of T_{AST} giving only a small error using grid cell size D. It is assumed that the same analysis in the full scale scenario would give the same results and that grid cell size D can be used.

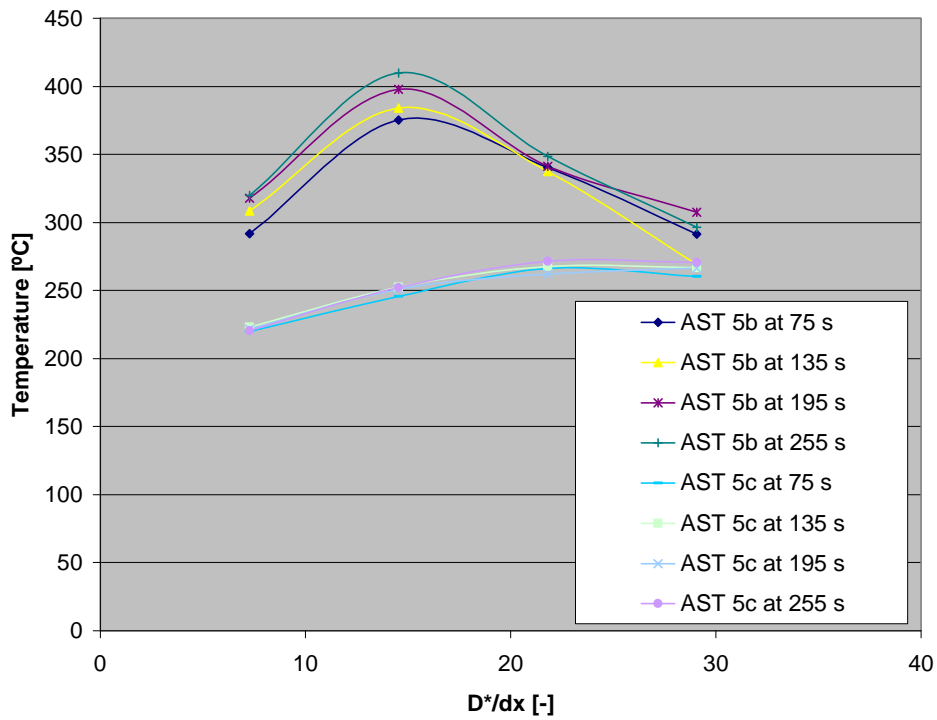


Figure 4-27 Grid cell size analysis in the mirrored symmetric model of AST at different time in the simulation.

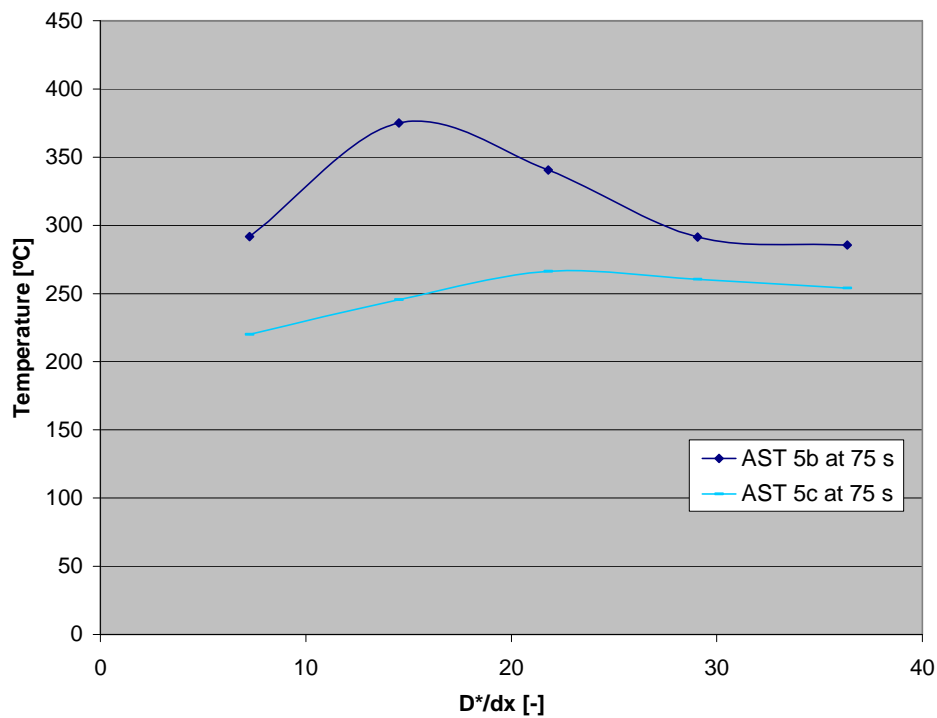


Figure 4-28 T_{AST} in simulation with grid cell size A to E at time 75 s.

4.4.2.3 Mirror function

When using the mirror function in simulations the computation cost is reduced to 50% since only half the test volume is calculated. To see if the feature can be used in this scenario two comparisons are being made between full scale symmetric simulations and mirrored ditto. These comparisons are made with grid cell size A and B in the primary mesh.

The first test is made to see if the calculated values from the reference points in the mirrored symmetry plane are similar to the values calculated one grid cell besides. This test is done to see if there is any deviation due to the mirror function or if the values from reference points in the symmetry plane can be used.

The test is made in a simplified model to save time (see Figure 4-29). A more specified view of the set up of reference points seen on the cross section is presented in Figure 4-30. Reference point c and d are located close to each other so that the calculated temperature differences between reference point c and d can be assumed to be very small. The calculations of T_{AST} in reference point c and d (see Figure 4-31) show a fairly good agreement. This indicates that reference points in the symmetry plane could be used.

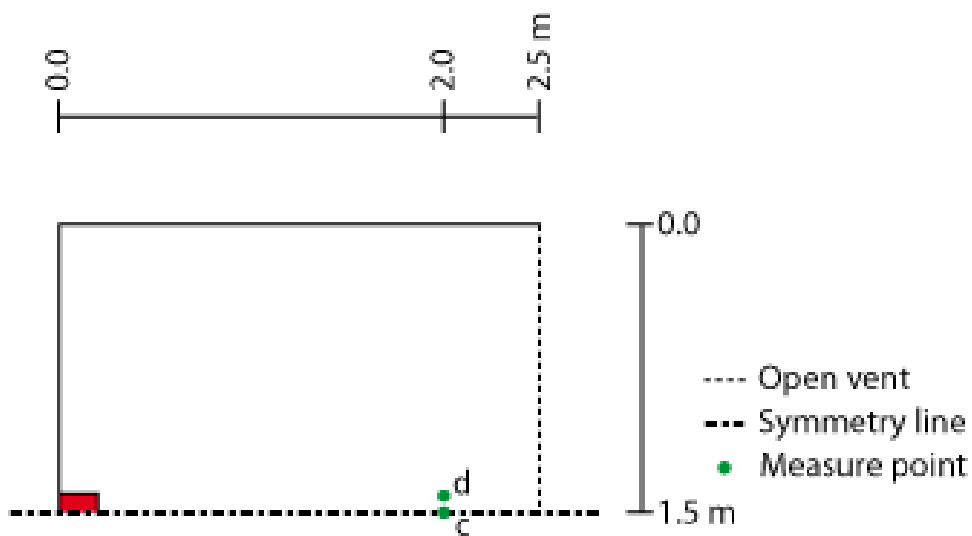


Figure 4-29 Simplified set up to compare the calculated values from reference points c and d. Red square represents energy source.

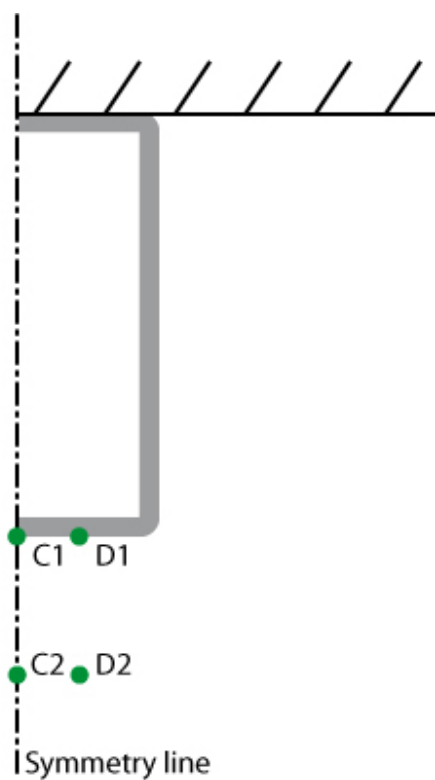


Figure 4-30 Reference points with measure devices in simulation controlling error in the mirror slice.

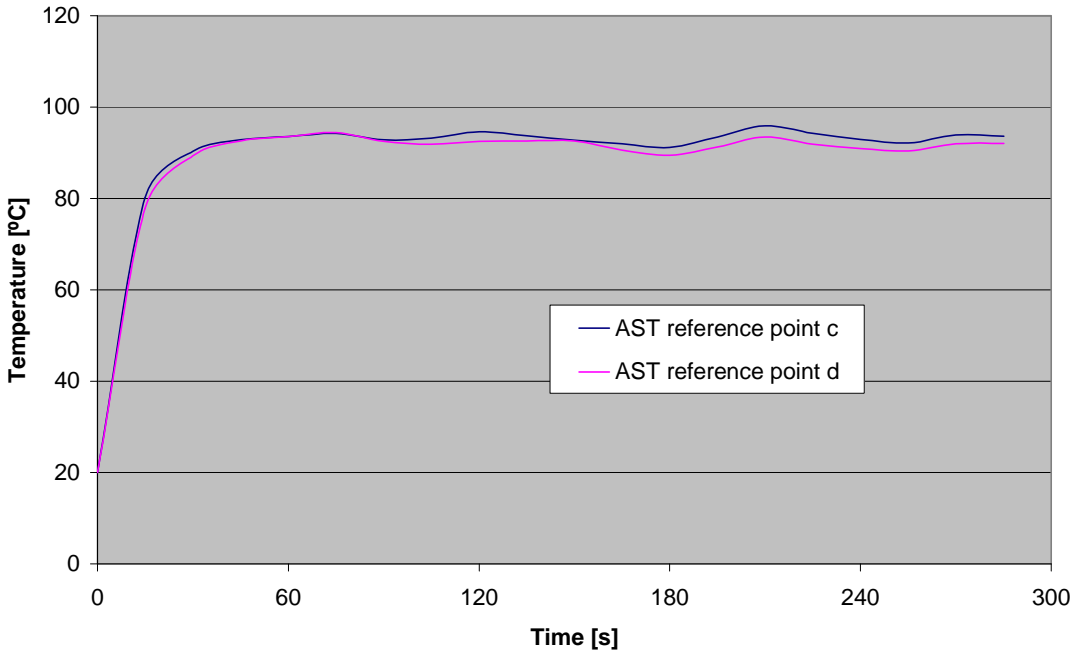


Figure 4-31 T_{AST} from reference point c and d.

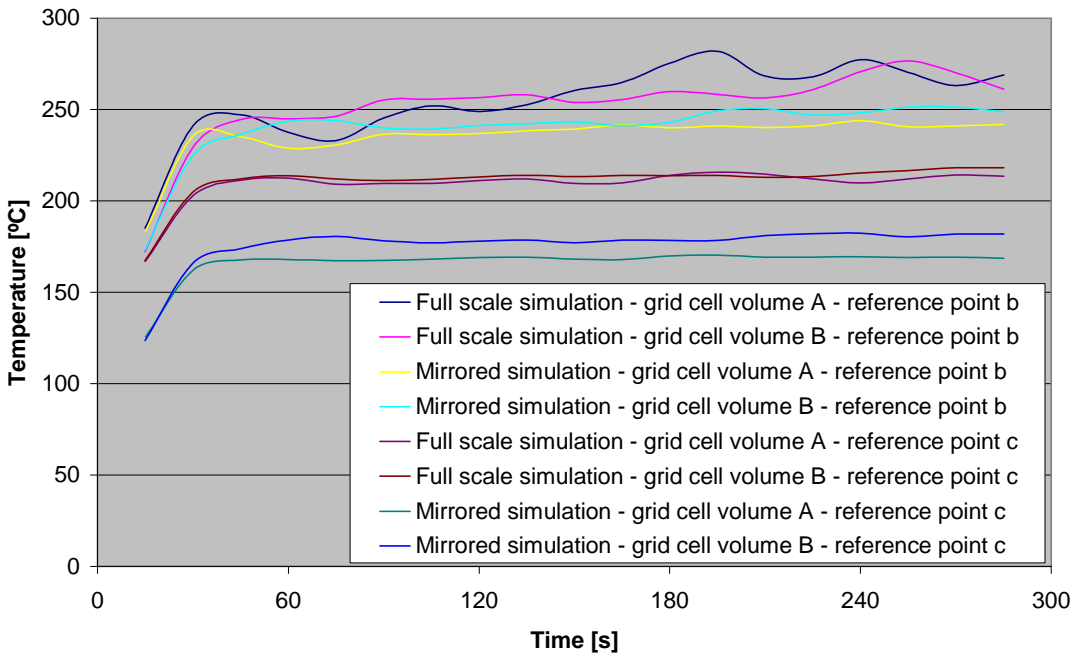


Figure 4-32 Differences between T_{AST} in the full scale and mirrored simulations.

The second test is used to compare the results between the symmetric mirrored and symmetric full scale simulation. Figure 4-32 showing that the mirrored

simulation gives a fair representation of temperatures from the full scale simulation in reference point b but deviates 25 % in reference point c.

This indicates that the mirror function gives reasonable results at some distance from the symmetry line. However it is not advised to use the results from reference points on the symmetry line in comparison to full scale experiments. This can be explained with turbulence which is not symmetric and therefore is difficult to deal with close to the symmetry line.

4.4.2.4 Measure devices outside the primary mesh

Since the primary mesh only cover reference set 5 and 6 a complementary test is made to see if the output from the reference points outside the primary mesh can be used. To test this, results from reference set 4 in simulations with a primary mesh of dimensions shown in Figure 4-25 with grid cell size B are compared to a simulation with the same grid cell size but an extended primary mesh including reference set 4 (see Figure 4-33).

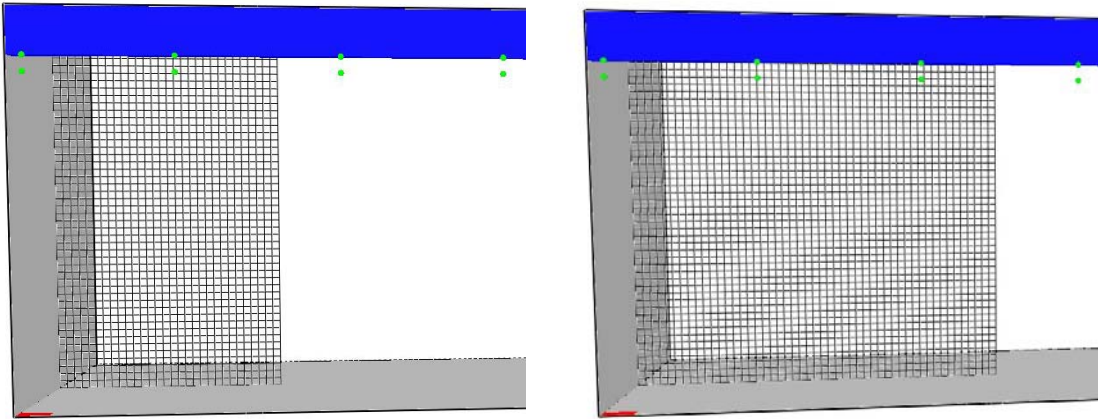


Figure 4-33 Primary mesh as defined in Figure 4-25 and extended primary mesh.

The results from these simulations are shown in Figure 4-34. The deviation is small and it is assumed that these results can be used although results from one single mesh have higher accuracy [2].

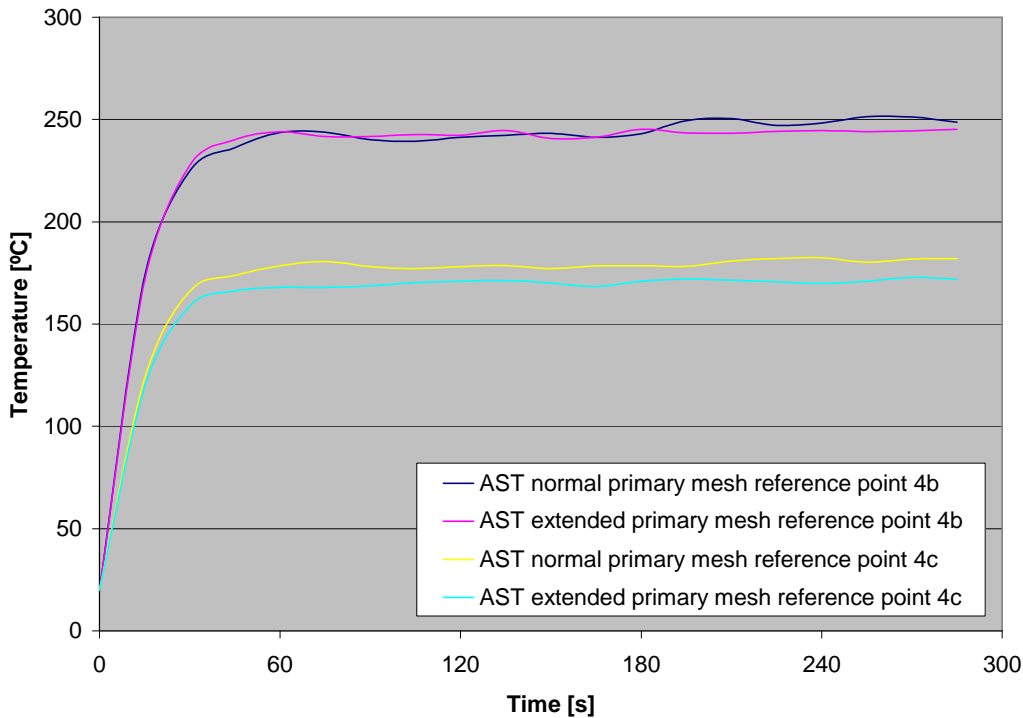


Figure 4-34 Values from reference set 4 with different sized primary mesh.

4.4.3 Experimental set up that can be verified

4.4.3.1 Geometry

The scenario used in the experimentally verifiable set up is a beam placed in a furnace for Room Corner Tests of dimensions 3.6 m x 2.4 m x 2.4 m. The beam used will be a RHS200 beam with the dimensions 200 mm x 100 mm and a thickness of 8 mm. The beam and energy source is set up centred as in the symmetric case with the difference that the top surface of the beam in this scenario is located 0.1 m below the ceiling (see Figure 4-35). The energy source is set to 500 kW.

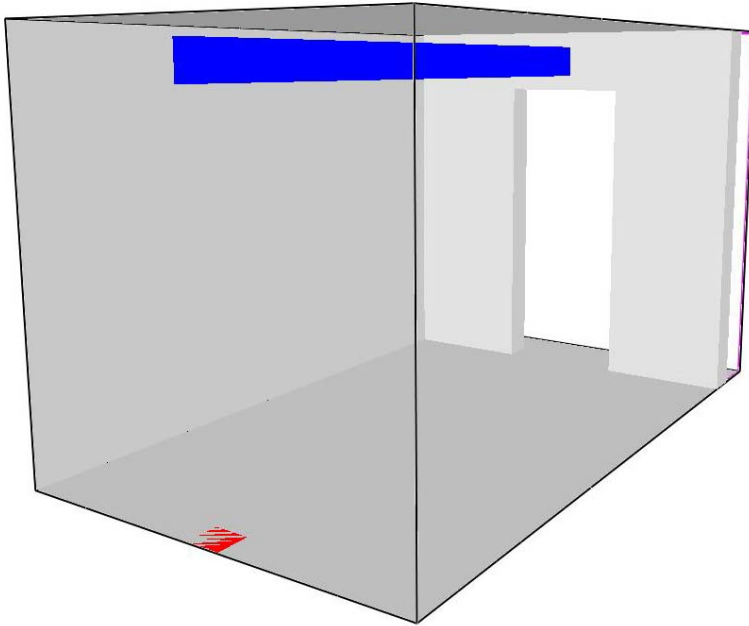


Figure 4-35 Set up of experimentally verifiable model.

4.4.3.2 Mesh

In Figure 4-36 is the numbering of meshes. The primary mesh is extended over three reference sets to provide more output data with high reliability. The grid sizes used in the different meshed can be seen in Table 4

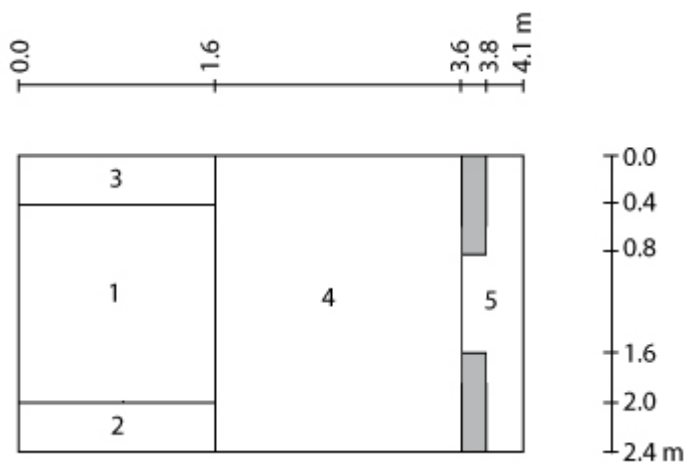


Figure 4-36 Mesh set up in experimentally verifiable model. The heat source is located in mesh 1.

Table 4 Grid cell size of different meshes in the experimentally verifiable model.

Mesh	Grid cell size [cm]	$\frac{D^*}{\delta x}$
1	2.5 x 2.5 x 2.5	29.08
2	5 x 5 x 5	14.54
3	5 x 5 x 5	14.54
4	5 x 5 x 5	14.54
5	10 x 10 x 10	7.27

reference points are located in sets at the distances of 0.1, 0.8, 1.5, 2.2, 2.9 and 3.5 m from the inner wall. Each set consists of 24 measure points located around the cross section of the beam on the centre of each side (see Figure 4-37).

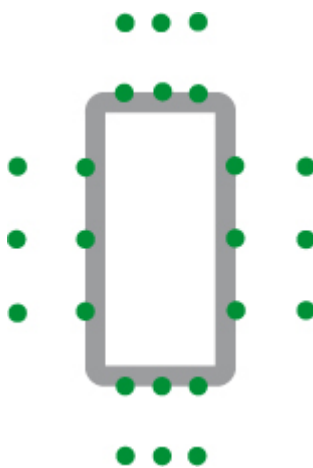


Figure 4-37 Reference points at each reference set in the experimentally verifiable set up.

The reference points located on the beam surface consists of measure devices for:

- ADIABATIC_SURFACE_TEMPERATURE
- WALL_TEMPERATURE
- HEAT_FLUX
- RADIATIVE_FLUX

- CONVECTIVE_FLUX
- RADIOMETER

The reference points not located on the beam surface consists of measure devices for:

- TEMPERATURE
- VELOCITY

The FDS-code for this simulation is in Appendix B.

5 Conclusions and further research

The general idea of simulating an image of the “real” fire environment surrounding construction elements with the use of T_{AST} works. The temperatures calculated will not always be absolutely correct and therefore still some research is needed in order to understand how to fully use AST.

Regarding the simulations in TASEF the major concern is the choice of the magnitude of the convection heat transfer coefficient. To be able to approximate the constant value used in TASEF it is necessary to get a reliable value on h . An output option in FDS giving h over time in every measure point specified could solve some of this problem. This could also solve the problem of transferring results between different beam set ups.

There is also a problem in understanding which simulation input to use in the beam in cases such as backing, material properties etc. An interesting idea would be to create a standardized beam to use in the simulation with results that are easy to translate to other kinds of beams. In converting the results analytically it is preferred to know as much as possible about the properties of the beams in the simulations. In this way at least the standard beam would be thoroughly studied and compared to experiments and other simulation results.

Further research is needed to isolate and specify special cases where exceptions have to be done. There is also still much to be done in understanding and simplifying the use of translation coefficients between different cases.

It would be very interesting to see what the limitations are in the applicability of this theory. Convection is one area but are there any other aspects that require

more research in order to use FDS as a method for predicting thermal exposure from fires. Some areas that would be interesting to study further are:

- Conversion of convection heat transfer coefficient from the FDS calculations.
- Experimental comparison and understanding of results.
- Development of a standardized beam and methods to transfer the results with this beam in different simulations to other beams.
- Determination of largest difference in size between beams, truss compared to solid construction, conversion between different materials etc.
- Development of methods for using this technique in construction design.

To work with the interpretation of T_{AST} requires a very informed user until enough is done to facilitate the use in construction design. Even then it requires much in the set up of the fire scenario but as the knowledge increases in the area of fire simulations T_{AST} is the way to go.

Regarding the sensitivity analysis the test of the extended primary grid shows that it is possible to model measure devices in a coarser secondary grid. One thing that could not be tested due to lack of computer resources is the difference in size between the primary and secondary grid. The dimensionless grid cell size in test had a ratio of 2:1 in the grid transition showing good agreement. Hence the ratio between the primary and surrounding meshes are set to a ratio of 2:1.

References

- [1] www.nist.gov
- [2] McGrattan, K., Hostikka S., Floyd, J., Klein, B., (2007). *Fire Dynamic Simulator (Version 5) User's Manual*,
Gaithersburg, Maryland: National Institute of Standards and Technology,
Building and Research Laboratory
NIST Special Publications 1019-5
- [3] Ulf Wickström, senior researcher and manager of fire technology at SP
Swedish National Testing and Research Institute
Private communication
- [4] Wickström, U., (2007) *Methods for Predicting Temperature in Fire Exposed Structures*
Borås: SP Swedish National Testing and Research Institute,
SP Draft 2007
- [5] Holman, J.R., (1976). *Heat Transfer*, 4th Edition.
New York: McGraw-Hill
- [6] Drysdale, D., (1998). *An Introduction to Fire Dynamics, Second Edition*
Chichester: John Wiley & Sons, LTD
- [7] Magnusson, S.E., Thelandersson, S. (1970). Time – Temperature Curves
of Complete Process of Fire Development; Theoretical Study of Wood
Fuel Fires in Enclosed Spaces.
*Acta Polytechnica Scandinavica, Civil Engineering and Building
Construction Series No 65.*
- [8] EC 1., (2002). *Eurocode 1 – Actions on structures – Part 1-2: General
actions – Actions on structures exposed to fire.*
Brussels: European Committee for Standardization
- [9] EC 3., (2003). *Eurocode 3 – Design of steel structures – Part 1-2:
General rules – Structural fire design*
Brussels: European Committee for Standardization

- [10] EC 3., (2003). *Eurocode 3 - Design of steel structures – Part 1-1: General rules and rules for buildings*.
Brussels: European Committee for Standardization
- [11] McGrattan, K., Hostikka S., Floyd, J., Baum, H., Rehm, R., (2007). *Fire Dynamic Simulator (Version 5) Technical Reference Guide*,
Gaithersburg, Maryland: National Institute of Standards and Technology,
Building and Research Laboratory
NIST Special Publications 1018-5
- [12] Ottosen, N., Petersson, H., (1992) *Introduction to the Finite Element Method*
Harlow: Pearson Education Limited
- [13] Sterner, E. and Wickström, U., (1990) *TASEF - Temperature Analysis of Structures Exposed to Fire*,
Borås: Swedish National Testing and Research Institute,
SP Report 1990:05
- [14] Sterner, E., Wickström, U., (1990). *TASEF – Temperature Analysis of Structures Exposed to Fire – User’s Manual*,
Borås: Swedish National Testing and Research Institute:
SP Report 1990:05
- [15] Wickström, U., Pålsson, J., (1999). *Scheme for Verification of Computer Codes for Calculating Temperature in Fire Exposed Structures*
Borås: SP Swedish Testing and Research Institute,
SP Report 1999:36

Appendix A

INTASEF-file

```
NO
TT 0.00000E+00
Balk RHS300 Provning av Adiabatisk yttemperatur
F
0.30000E+00 0.40000E+00 0.30000E+00 0.40000E+00
4 6 11 0
F 0.00000E+00 0.30000E+00 0.30000E+00 0.40000E+00
T 0.10000E+00 0.00000E+00 0.30000E+00 0.30000E+00
T 0.00000E+00 0.95000E-02 0.90500E-01 0.29050E+00

0.25000E-01 0.50000E-01 0.75000E-01 0.15000E+00
0.20000E+00 0.25000E+00
0.50000E-01 0.75000E-01 0.10000E+00 0.12500E+00
0.15000E+00 0.17500E+00 0.20000E+00 0.22500E+00
0.25000E+00 0.32000E+00 0.34000E+00
19
1 2 0 0 0 0 0 0
17 18 0 0 0 0 0 0
33 34 0 0 0 0 0 0
49 50 0 0 0 0 0 0
65 66 81 82 0 0 0 0
67 83 0 0 0 0 0 0
68 84 0 0 0 0 0 0
69 85 0 0 0 0 0 0
70 86 0 0 0 0 0 0
71 87 0 0 0 0 0 0
72 88 0 0 0 0 0 0
73 89 0 0 0 0 0 0
74 90 0 0 0 0 0 0
75 91 0 0 0 0 0 0
92 93 77 76 0 0 0 0
60 61 0 0 0 0 0 0
44 45 0 0 0 0 0 0
28 29 0 0 0 0 0 0
12 13 0 0 0 0 0 0
STM2
F 3 7 0 0.10000E+01
0.00000E+00 0.60000E+02 0.80000E+03 0.27000E+02
0.20000E+04 0.27000E+02
0.00000E+00 0.00000E+00 0.20000E+03 0.21690E+06
0.40000E+03 0.46610E+06 0.60000E+03 0.75810E+06
0.70000E+03 0.92690E+06 0.80000E+03 0.111920E+07
0.12000E+04 0.17660E+07
STM1
T 4 7 0 0.10000E+01
0.25000E+02 0.18000E+01 0.11500E+03 0.12800E+01
0.80000E+03 0.80000E+00 0.12000E+04 0.52000E+00

0.00000E+00 0.00000E+00 0.10000E+03 0.55560E+05
0.11500E+03 0.91110E+05 0.20000E+03 0.12940E+06
0.60000E+03 0.39720E+06 0.10000E+04 0.69670E+06
0.15000E+04 0.10000E+07

0.20000E+02 0.20000E+02 0.56700E-07 0.27315E+03
7
1 3 0.80000E+00 0.25000E+02 0.10000E+01
1 17 33
2 4 0.80000E+00 0.25000E+02 0.10000E+01
33 49 65 81
3 5 0.80000E+00 0.25000E+02 0.10000E+01
81 82 83 84 85
4 5 0.80000E+00 0.25000E+02 0.10000E+01
85 86 87 88 89
5 5 0.80000E+00 0.25000E+02 0.10000E+01
89 90 91 92 93
6 5 0.80000E+00 0.25000E+02 0.10000E+01
93 109 125 141 157
7 19 0.80000E+00 0.25000E+02 0.10000E+01
2 18 34 50 66 67 68 69 70 71
72 73 74 75 76 60 44 28 12
6
1 1
2 2
3 3
4 4
5 5
6 6
```

```
0
0
VOIDS
1
T F 7 0 0 0
NO TUBE
21 0.7500E-01 0.7500E-01 0.9000E+00 10000 1
0.0000E+00 0.3750E-02 0.7500E-02 0.1500E-01 0.1875E-01 0.3200E-01
0.2250E-01 0.2625E-01 0.3000E-01 0.3375E-01 0.3750E-01 0.4125E-01
0.4500E-01 0.4875E-01 0.5250E-01 0.5625E-01 0.6000E-01 0.6375E-01
0.6750E-01 0.7125E-01 0.7500E-01
6
```

[Six different time - temperature curves]

Appendix B

FDS code

```
&HEAD      CHID = 'Final_rct'
           TITLE = 'Simulering 1' /

&MESH      IJK = 64,64,96
           XB = 0.4,2.0,2.5,4.1,0.0,2.4 /
&MESH      IJK = 8,32,48
           XB = 0.0,0.4,2.5,4.1,0.0,2.4 /
&MESH      IJK = 8,32,48
           XB = 2.0,2.4,2.5,4.1,0.0,2.4 /
&MESH      IJK = 48,40,48
           XB = 0.0,2.4,0.5,2.5,0.0,2.4 /
&MESH      IJK = 24,5,24
           XB = 0.0,2.4,0.0,0.5,0.0,2.4 /

&TIME      TWFIN = 10. /

&MISC      SURF_DEFAULT = 'WALL'
           RESTART = .FALSE. /

&DUMP      DT_RESTART = 15. /

&SURF      ID = 'FIRE'
           COLOR = 'RED'
           HRRPUA = 12500. /

&OBST      XB = 1.1,1.3,3.9,4.1,0.0,0.0, SURF_ID='FIRE'

&MATL      ID = 'CONCRETE'
           SPECIFIC_HEAT = 1000.
           CONDUCTIVITY = 0.5
           DENSITY = 800.
           EMISSIVITY = 0.8 /

&SURF      ID = 'WALL'
           MATL_ID = 'CONCRETE'
           COLOR = 'SILVER'
           THICKNESS = 0.2 /

&OBST      XB = 0.0,2.4,0.3,0.5,0.0,2.4, SURF_ID='WALL' /
&HOLE      XB = 0.8,1.6,0.2,0.6,0.0,2.0 /
&VENT      MB = 'YMIN', SURF_ID='OPEN' /
&VENT      XB = 0.0,0.0,0.0,0.3,0.0,2.4, SURF_ID='OPEN' /
&VENT      XB = 2.4,2.4,0.0,0.3,0.0,2.4, SURF_ID='OPEN' /
&VENT      XB = 0.0,2.4,0.0,0.3,2.4,2.4, SURF_ID='OPEN' /

&MATL      ID = 'STEEL'
           FYI = 'EUROCODE'
           CONDUCTIVITY_RAMP = 'K_RAMP'
           SPECIFIC_HEAT_RAMP = 'C_RAMP'
           DENSITY = 7850. /
&RAMP      ID = 'K_RAMP', T= 20., F= 54. /
&RAMP      ID = 'K_RAMP', T=800., F= 27. /

&RAMP      ID = 'C_RAMP', T= 20., F=0.425 /
&RAMP      ID = 'C_RAMP', T=600., F=0.666 /
&RAMP      ID = 'C_RAMP', T=738., F=1.0 /
&RAMP      ID = 'C_RAMP', T=900., F=0.650 /

&SURF      ID = 'RHS200'
           MATL_ID = 'STEEL'
           COLOR = 'BLUE'
           THICKNESS = 0.008 /

&OBST XB = 1.15,1.25,0.5,4.1,2.1,2.3, SURF_ID='RHS200' /

&DEVC      XYZ = 1.150,4.0,2.15, IOR=-1, ID='AST_1a', QUANTITY='ADIABATIC_SURFACE_TEMPERATURE' /
&DEVC      XYZ = 1.150,4.0,2.20, IOR=-1, ID='AST_1b', QUANTITY='ADIABATIC_SURFACE_TEMPERATURE' /
&DEVC      XYZ = 1.150,4.0,2.25, IOR=-1, ID='AST_1c', QUANTITY='ADIABATIC_SURFACE_TEMPERATURE' /
&DEVC      XYZ = 1.250,4.0,2.15, IOR= 1, ID='AST_1d', QUANTITY='ADIABATIC_SURFACE_TEMPERATURE' /
&DEVC      XYZ = 1.250,4.0,2.20, IOR= 1, ID='AST_1e', QUANTITY='ADIABATIC_SURFACE_TEMPERATURE' /
&DEVC      XYZ = 1.250,4.0,2.25, IOR= 1, ID='AST_1f', QUANTITY='ADIABATIC_SURFACE_TEMPERATURE' /
&DEVC      XYZ = 1.175,4.0,2.10, IOR=-3, ID='AST_1g', QUANTITY='ADIABATIC_SURFACE_TEMPERATURE' /
&DEVC      XYZ = 1.200,4.0,2.10, IOR=-3, ID='AST_1h', QUANTITY='ADIABATIC_SURFACE_TEMPERATURE' /
&DEVC      XYZ = 1.225,4.0,2.10, IOR=-3, ID='AST_1i', QUANTITY='ADIABATIC_SURFACE_TEMPERATURE' /
&DEVC      XYZ = 1.175,4.0,2.30, IOR= 3, ID='AST_1j', QUANTITY='ADIABATIC_SURFACE_TEMPERATURE' /
&DEVC      XYZ = 1.200,4.0,2.30, IOR= 3, ID='AST_1k', QUANTITY='ADIABATIC_SURFACE_TEMPERATURE' /
```



```
&SLCF XB = 0.0,3.0,5.9,5.9,0.0,2.5, QUANTITY='VELOCITY', VECTOR=.TRUE. /
&SLCF XB = 0.0,2.4,0.0,4.1,2.2,2.2, QUANTITY='VELOCITY', VECTOR=.TRUE. /

&BNDF QUANTITY = 'WALL_TEMPERATURE' /
&BNDF QUANTITY = 'HEAT_FLUX' /

&TAIL /
```